Vrije Universiteit Brussel

Vrije Universiteit Brussel

Faculteit Toegepaste Wetenschappen
Vakgroep Toegepaste Natuurkunde en Fotonica

Universidad Pública de Navarra

upna Universidad Pública de Navarra Nafarroako Unibertsitate Publikoa

Escuela Técnica Superior de
Ingenieros Industriales y de Telecomunicación

STUDY OF LIGHT PROPAGATION IN LIQUID CRYSTAL OVERLAYING VERTICAL-CAVITY SURFACE-EMITTING LASER

Sara Pardo Fanlo

Academic year: 2010-2011

Promotors: Prof. Dr. Krassimir Panajotov
Prof. Dr. Mikel Arizaleta
Prof. Dr. Joaquín Sevilla

Acknowledgements

This work would not have been completed without help and support of many individuals. I am highly grateful to all of them. Moreover, this is the last step of my graduate education and many people have been a part of it. I would like to thank everyone who has helped me along the way.

First of all, I would like to thank Prof. Krassimir Panajotov for providing me the opportunity to conduct my work under him and for his guidance and support over the course of it. I also want to thank Veena, Etienne and Mateusz. It has been a pleasure working and learning with you in the lab.

Si hay alguien a quien debo agradecer su ayuda es Mikel Arizaleta. Por su apoyo, sus consejos y su infinita paciencia. Por resolver mis dudas y animarme tanto. Seguir sus pasos me ha hecho ver lo buen ingeniero que es; él me ha demostrado que es mejor persona. Has conseguido motivarme en todas nuestras conversaciones y siento no haber estado a la altura. Gracias por ser mucho más que un tutor para mí.

Quiero darle las gracias a Joaquín Sevilla, por sus palabras de ánimo, su ayuda y sinceridad.

Gracias a mis cinco biólogas por ofrecerme divertidísimos momentos de desconexión, soportarme y escucharme durante estos nueve meses que tan duros me han resultado. Por recibirme siempre con una sonrisa y seguir contando conmigo pese a que apenas os hiciera caso. Tenéis una amiga para siempre.

A mi familia, especialmente a mis padres y hermanos. Desde el principio habéis creído que éste era un mundo de locos pero habéis confiado en mí, apoyándome a lo largo de todo el camino. Sólo puedo daros las gracias. Por todo; por vuestra ayuda, preocupación y paciencia. He aprendido mucho de vosotros y os debo gran parte de lo que soy. Gracias por estar ahí en todo momento.

No puedo olvidarme de toda la gente que he conocido en Pamplona y que ha formado parte de mi aventura universitaria en mayor o menor medida.

A mis compañeras de piso, que han sido mi pequeña familia y con las que tantas cosas he vivido. Me llevo infinidad de anécdotas y recuerdos. Nos hemos ayudado y apoyado mutuamente. Ya os echo de menos...

A mis amigos y compañeros en teleco que han contribuido a que todo esto fuera más fácil. Apuntes, trabajos, presentaciones, agobios, exámenes, ratos de biblioteca, horas de comedor, descansos… Risas, cotilleos, largas conversaciones, juergas, Carpas, Semanas del Pintxo, el viaje a Madrid, quedadas sanfermineras… Son innumerables los buenos momentos que nunca olvidaré.

Nada hubiera sido lo mismo sin Ainhoa. Han sido muchas horas juntas de llorar y reír, sufrir e ilusionarnos, codo con codo, compartiendo un objetivo común. Ahora está más cerca. Eres una persona genial y estoy convencida de que vas a ser mejor ingeniera. Gracias por convertirte en alguien tan especial en mi vida.

También quiero acordarme de Sergio, a quien le debo tanto… Gracias por todo tu apoyo. Por confiar en mí, por escucharme, por entenderme, por tus palabras bonitas en mis momentos de bajón, por tu sentido del humor y por todo lo que has aportado, no sólo a mi carrera, sino a mi vida entera. Siempre tendré un hueco para ti.

A Marta, por su ayuda y apoyo incondicionales. Por admirarme sin ningún motivo. Por soportarme y comprenderme. Por todo lo que hemos pasado juntas que a veces nos ha distanciado un poco, para luego unirnos más que antes. Pero, sobre todo, porque pase lo pase siempre estás a mi lado. Gracias.

Finalmente, gracias a ti, Javi. Por todo tu esfuerzo y dedicación ayudándome. Por tu ilusión y tu alegría. Por considerarme la mejor y no dudar nunca de mi capacidad. Por anteponer mis problemas a todo lo demás. Y por tantas otras cosas… Ha sido un año muy duro y no habría podido llegar hasta aquí sin ti. Gracias por todo; sobre todo, por esa eterna sonrisa que te hace único.

Sara Pardo Fanlo

Bruselas, mayo de 2011.

Contents

Chapter 1

Introduction

1.1 Basic concepts of semiconductor lasers

Semiconductor lasers have been developed extensively because of their importance for optical communications. They are also known as laser diodes or injection lasers, and their properties have been deeply studied and discussed.

Atoms and molecules have discrete levels of energy. When they assemble to build more complex structures, they interact and the higher levels of energy form separated energy bands. The space between the last band plenty of electrons (valence band) and the top band that could be occupied or not (conduction band) determines the electric properties of the material. We can differentiate between the behaviour of metals, semiconductors and dielectrics.

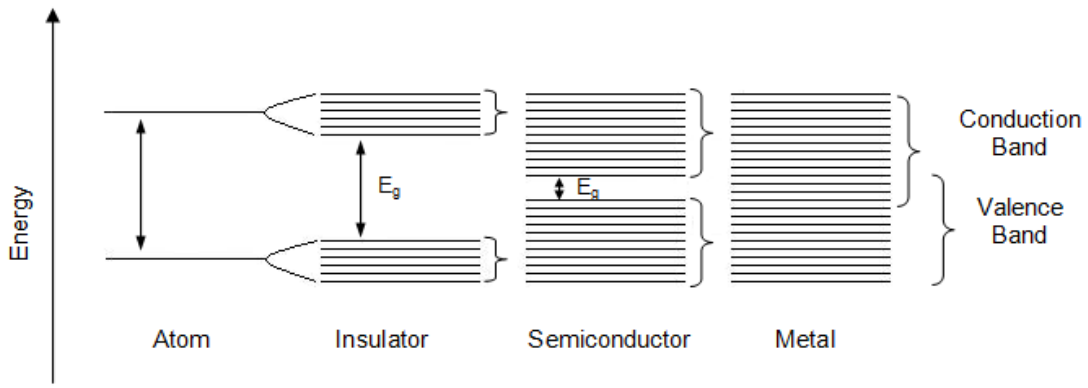

Figure 1.1: *Energy levels for an atom, an insulator, a semiconductor and a metal. E_g is the energy gap between the valence and conduction bands for each material. There is not gap in conductor, the bands overlap.*

The probability of occupancy of the different states is given for the Fermi-Dirac distribution where E_F is called the Fermi level, T is the temperature and k is the Boltzman constant [1]. At the Fermi level of energy, $E = E_F$, the probability is one-half.

$$f(E) = \frac{1}{1 + e^{\left(\frac{E - E_F}{kT}\right)}}$$

The gap between both bands is lower for semiconductors than for insulators. Therefore, by increasing the temperature a small group of electrons moves to the conduction band. Consequently, the same number of electronic holes is produced in the valence band. Both are charge carriers and take part in the conduction process. When one electron jumps to a higher level of energy leaving a hole, makes possible the movement of another electron to fill this hole. Adding thermal energy enough, the number of electrons and holes is raised and the material conductivity is increased.

The band gap of a semiconductor is one of two types, a direct band gap or an indirect band gap. The minimal-energy state in the conduction band, and the maximal-energy state in the valence band, are each characterized by a certain k-vector. If the k-vectors are the same, it is called direct gap. If they are different, it is called indirect gap. For having a successful interaction of the pairs with photons with the proper energy, it is necessary to conserve the energy and momentum [1].

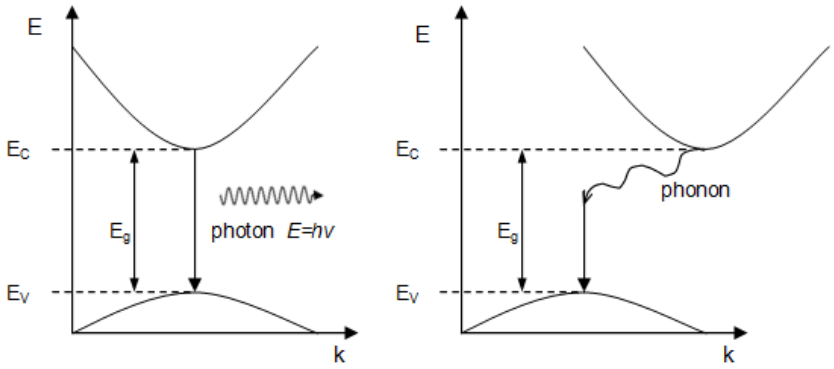

Figure 1.2*: Energy vs. momentum for a semiconductor with direct band gap (left) and with indirect band gap (right). The change of momentum in indirect gap semiconductors implies the generation of a phonon.*

Considering only the limited number of pairs of levels from these bands for a given transition energy, we can see four basic mechanisms of electronic recombination/generation (photon emission/absorption):

1. Spontaneous recombination (photon emission): An electron goes from the conduction band to the valence band and recombines with a hole. A photon with random phase and direction is generated. The emission of such a large number of theses photons would be incoherent. The system goes to a lower state of energy.

2. Stimulated generation (photon absorption): The energy of one incident photon is absorbed by the material. An electron jumps to the conduction band leaving a hole in the valence band. The system changes to a higher energy state.

3. Stimulated recombination (coherent photon emission): The absorption of one photon stimulates the recombination of an electron-hole pair, while a new photon is generated. This photon has the same frequency, direction of propagation and phase as the stimulated photon.

4. Nonradiative recombination: The recombination of one electron of the conduction band and one hole of the valence band doesn't generate useful photons. The energy is dissipated as heat.

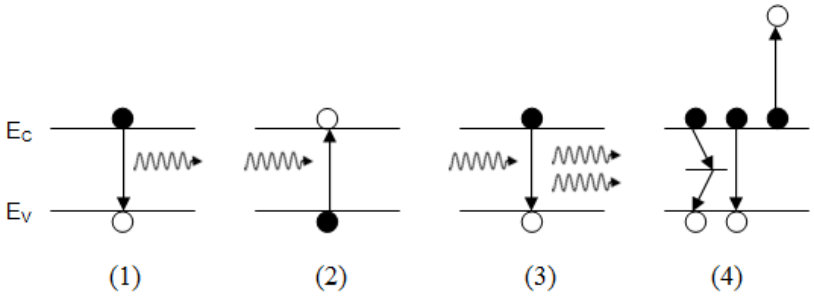

Figure 1.3: *Possible electronic transitions and interactions with ligthwaves in a semiconductor.*

Semiconductors conductivity depends on the number of carriers and their mobility. An intrinsic semiconductor is a semiconductor with the same number of electrons and holes. In these materials, the only way to control the concentration of electrons and holes

to generate photons is setting the temperature. Adding impurities to the intrinsic semiconductor, the conductivity can be improved. The doped material obtained is an extrinsic semiconductor. By doping it with impurities whose atoms have one more electron than the semiconductor material, the semiconductor is called n-type. The Fermi level, lying in the middle of the band gap for intrinsic semiconductors, moves toward the conduction band as the dopant concentration increases. If the atoms have one less electron, the semiconductor is called p-type. Similarly, the Fermi level moves toward the valence band for p-type semiconductors and lies inside it under heavy doping. In thermal equilibrium, the two Fermi levels coincide ($E_{FC} = E_{FV}$). They can be separated by dumping energy into the semiconductor from an external energy source. The most convenient way for pumping a semiconductor is to use a forward-biased p–n junction.

A laser emits light through a process of optical amplification based on the stimulated emission of photons. It is necessary to have an active medium where the stimulated recombination dominates providing gain and a cavity to get an optical feedback.

For semiconductor lasers, the active medium is a semiconductor material. Stimulated emission can dominate only if the condition of population inversion is satisfied. It is necessary to inject many electrons and holes in order to have the Fermi level separation exceeding the band gap. The p-n junction has to be under forward biasing. It starts emitting incoherent light until certain value of the injection carrier density. At that point, population inversion exists in the active medium and there is an optical gain.

That optical gain alone is not enough for laser oscillation. An optical feedback is also necessary. For semiconductor lasers emitting from the edge, the cavity is not built with external mirrors because the two cleaved laser facets act as mirrors.

Some photons generated by stimulated emission are lost because of cavity losses. If the optical gain is not big enough to compensate the cavity losses, the photon population cannot build up. Thus, a minimum amount of gain is necessary for the laser operation. This amount can be realized only when the laser is pumped over the threshold level.

1.2 Vertical Cavity Surface Emitting Lasers (VCSELs)

Vertical-Cavity Surface-Emitting lasers have the resonant cavity normal to the substrate so they emit light in a direction perpendicular to the active-layer plane.

They have a vertical structure of thin layers where the active region is sandwiched between two high reflectivity Distributed Bragg Reflectors (DBR) [2]. The structure is built by growing the layers with epitaxial techniques. There are different kinds of structures developed to obtain the vertical confinement.

The extremely short cavity makes the single mode emission possible as the frequency spacing between the longitudinal modes exceeds the gain bandwidth.

The beam of the light emitted is circular and can be coupled into a fiber with high efficiency.

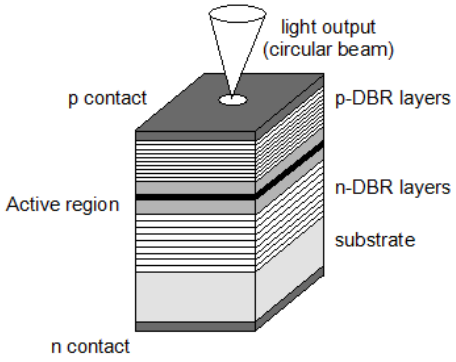

Figure 1.4: *Vertical Cavity Surface Emitting Laser.*

An entire two-dimensional array of VCSELs can be manufactured to use in optical computing. Also, one array can be tested during the production process without requiring separation of lasers due to the vertical light emission. Thus, the cost of a VCSEL can be much lower than that of other types of lasers.

These properties result in a number of advantages that are leading to rapid adoption of VCSELs for lightwave communications. However, they have some disadvantages comparing to other lasers: less maximum single transverse-mode power emission, problems to work at 1310 or 1550 nm and its non stable polarization.

1.3 Polarization properties of VCSELs

The polarization direction of the emitted light by a VCSEL is not defined in the manufacturing process. Its polarization is not defined a priori due to the cylindrical symmetry of the cavity and the emitting direction that is perpendicular to the active layer. Nevertheless, VCSELs emit linearly polarized light because of the birefringence introduced by non intentional stress during the production of the lasers and because of the electro-optic effect in the cavity and the mirrors [3].

The two preferred polarization directions of the fundamental transverse mode are along the [110] and [1-10] crystal axes in VCSELs grown on [001] oriented substrate plane [4]. These two orthogonal linear polarization modes are strongly anticorrelated. The birefringence of the cavity makes them to have a small difference between their wavelengths.

The anisotropy introduced in the manufacturing process is not predictable. Therefore, the polarization of the fundamental mode can not be predicted and varies from one VCSEL to another. The linearly polarized mode of emission can change between these two orthogonal states when changing the temperature or increasing the injection current. This polarization switching has been explained by several physical mechanisms. It is possible to switch from shorter to longer wavelength mode or from longer to shorter [5].

1.4 Effect of optical feedback on VCSEL properties

When the light emitted by a laser finds an obstacle (like the facet of a fiber), a reflection is generated. A portion of the light goes back to the laser and enters into the cavity with a time delay. This optical feedback can modify the laser behaviour [6].

VCSELs have a very high reflectivity of the mirrors that should not make them vulnerable to the optical feedback effects. However, they are as sensitive to feedback as edge emitting lasers because of the very short cavity [7]. The effects of dynamical regimes of feedback have been observed in the spectrum.

According to the amount of light that re-enters into the laser, it is possible to observe complicated dynamics like mode hopping, oscillatory and chaotic regimes. As the feedback increases, the emission spectrum gets broader [8].

The dynamics observed are also determined by the length of the external cavity considering the relation between the round trip time and the relaxation oscillation frequency of the laser.

1.5 Extremely short external cavity optical feedback

We talk about extremely short external cavity when the round trip time is much shorter than the relaxation oscillation period of the laser. The use of micro optic devices that can be affected by optical feedback from very short external cavities is increasing. It is common to place the laser close to the next element in the system, only separated by micrometers. Thus, the study of the ESEC optical feedback effects on the lasers behaviour is very important [9].

1.6 Introduction to Liquid Crystals

The transition from one physical state of matter to another is defined by a temperature value. Increasing the temperature, most of the solid crystals become liquids by melting. However, this is not the behaviour of all the substances. There are some organic materials which go through an intermediate phase. Liquid crystals are a state of matter that has properties between those of a conventional liquid and those of a solid crystal. They flow like liquids but their molecules have lost their positional order, while maintaining orientational order [10].

These intermediate phases in which liquid crystals could exist are mesophases, and the liquid crystal is a mesogen material. They are uniform phases that share the anisotropy of solids with the fluidity of liquids.

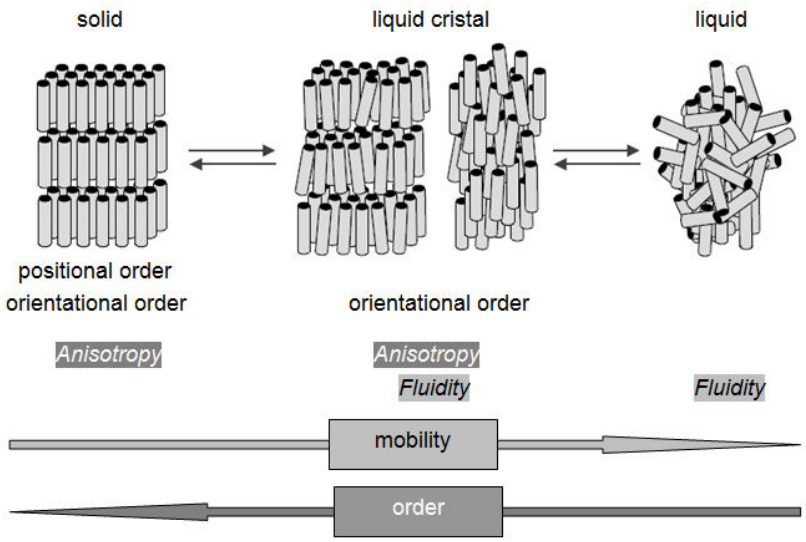

Figure 1.5: *Liquid crystal as another state of matter.*

According to the physical parameters controlling the existence of the liquid crystalline phases, liquid crystals can be divided into three distinctive types: thermotropic, lyotropic and polymeric phases.

Lyotropics are obtained when an appropriate concentration of a material is dissolved in some solvent. A compound, which has two immiscible hydrophilic and hydrophobic parts within the same molecule, is called an amphilic molecule. The concentration is the most important variable to determinate the existence of the liquid crystalline phase. Lyotropic liquid crystals have many biological applications [11].

Polymeric liquid crystals are materials that incorporate mesogenic groups in their polymer chains. They combine the properties of polymers with the anisotropic properties of liquid crystals. Depending on the degree of flexibility, there are three types of polymers. The most rigid is polypeptide chain, then the semirigid Dupont Kevlar and the most flexible, the vinyl [12]. They have more viscosity than the monomers and their main application is the optical storage.

A liquid crystal is thermotropic if the order of its components is determined or changed by temperature. It is possible to represent their molecular structure as discs or as rods, according to the main types of molecules that form the compound. We can distinguish three classes of thermotropics: nematics, cholesterics and smectics.

Thermotropic liquid crystals are the most used and studied because their optical properties. Therefore, they have many applications in electrooptics.

1.7 Nematics, Cholesterics and Smectics

In a nematic phase, the molecules have not positional order, but they are aligned in a general direction defined by the director axis. Although the molecules are free to flow because they are randomly distributed as in a liquid, they maintain their long-range directional order parallel to the director vector. The fluidity of nematics is similar to that of liquids but they can be easily aligned by an external magnetic or electric field.

Smectic liquid crystals have positional order. The molecules are oriented along one direction forming different layers according to the position of the molecules that form a pattern. There are several subphases of smectics depending on the arrangement and properties of the molecules.

Cholesteric phase is also called chiral nematic phase because of the chiral nature of its molecules. There is a twisting of the molecules perpendicular to the director, with the molecular axis parallel to the director. Thus, the molecules tend to have a helical alignment. For each plane, the director axis twists helicoidally around another perpendicular axis. So, we can consider these liquid crystals a variant of nematics made of nematic planes stacked.

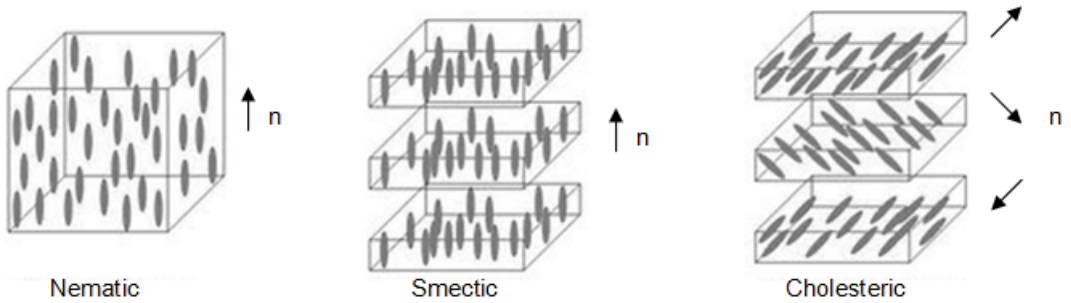

Figure 1.6: *Molecular alignments in liquid crystals.*

1.8 Nematic Liquid Crystals

Nematics are used in electro-optical devices very often [13]. The physical behaviour of nematics is very similar to the liquid one. It is necessary to work with flat thin cells containing the liquid crystal to appreciate its crystalline properties. The cell walls control the alignment of the axis in the liquid crystals. The two more common alignments for nematics are homogeneous or planar and homeotropic.

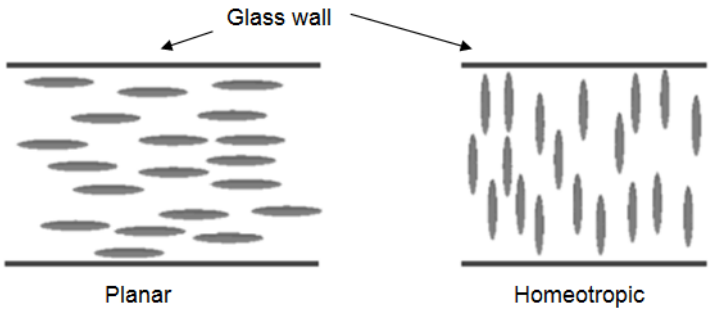

Figure 1.7: *Alignments for nematic cells.*

The dielectric constants, the refractive indices and the electrical conductivities characterize the electronic responses of liquid crystals to externally applied fields that can be electric, magnetic or optical [14]. The responses change depending on the field frequency and direction. We can distinguish two frequency regimes to study the electrooptical parameters: dc and low frequency, and optical frequency.

The conductivity anisotropy and an applied dc electric field can originate a space charge accumulation and a very strong reorientation of the director axis. When the permittivity along the director axis, $\varepsilon_{\parallel}$, is bigger than the one perpendicular to it, $\varepsilon_{\perp}$, nematics have positive anisotropy (dielectric anisotropy). This is the case of the majority of nematics. Other nematics have negative anisotropy ($\varepsilon_{\parallel} < \varepsilon_{\perp}$).

Organic liquids are dielectric. However, liquid crystals have some impurities that give rise to their conductivities. In general, $\sigma_{\parallel} > \sigma_{\perp}$. They can also vary using appropriate dopants. The electrical conductivity is very important in liquid crystals applications because it has influence in the stability, chemical degradation and lifetime of the devices.

In the optical regime, there is positive anisotropy ($\varepsilon_{\parallel} > \varepsilon_{\perp}$). Nematic crystals have a large birefringence through the whole optical spectral regime. Due to their importance for applied electrooptics devices, there are many studies about the two main refractive indices $n_{\parallel}$ and $n_{\perp}$ of an uniaxial liquid crystal and the anisotropy $n_{\parallel}$ - $n_{\perp}$.

1.9 Optics and Electro-Optics

It is possible to control and change the alignment of the anisotropic liquid crystal axis applying an externally field. Thus, the refractive index and phase shift that the light experienced going through the liquid crystal can be controlled.

As liquid crystals have a high birefringence and they are very susceptible to perturbations coming from external fields, applying a small voltage to a thin layer is enough to create the phase shift. The power consumed by the electrooptical process is very little because the interaction of the field with the nematic is dielectric, without current flow or energy dissipation. That is why liquid crystals are so demanded in optical displays, switching, information and image processing devices.

Polarized light incident on one crystal experiences different refractive indices depending on its states of polarization because crystals are optically anisotropic. We can speak about indices n_1, n_2, and n_3 for light polarized along the *x*, *y* and *z* axis. Light with an arbitrary polarization propagating in a crystal without relative orientation to the polarization direction has a complex result that involves all the indices. However, the crystal is usually cut or oriented with one plane coinciding with one polarization vector and the propagation direction. It is common to choose the *z* axis as an axis of symmetry. The polarization vector of the light propagating along this axis is perpendicular to that axis of symmetry, so the field lies on the *x*-*y* plane. If n_1 is not equal to n_2, the crystal is biaxial, whereas the crystal is called uniaxial when $n_1=n_2$. If $n_3>n_1,n_2$, the crystal is positive uniaxial or biaxial. On the other hand, if $n_3<n_1$, n2, it is negative uniaxial or biaxial.

Nematic liquid crystals are uniaxial ($n_1=n_2$). These indices are denoted as n_0 and n_3 is denoted as n_e. This denotation is referred to the extraordinary and ordinary components

if we study the propagation of the light in a birefringent crystal using the index ellipsoid method.

The refractive indices change when an external field is applied to a nematic liquid crystal due to the reorientation of the director axis. The orientation of the molecules in a liquid crystal is strongly altered applying a field. This alters the optical properties of it. The electrooptical devices that use liquid crystals combine it with other optical elements to control, modulate or switch the light. Its operation is based on those changes of optical properties.

The nematic liquid director axis responds to the field depending on the dielectric anisotropy. The director axis tends to align along the electric field for positive uniaxial liquid crystals ($n_e > n_o$). For negative uniaxial liquid crystals, the director axis tilts away from the electric field. It is possible to use positive uniaxial nematic liquid crystal with planar alignment and negative uniaxial nematic liquid crystal with homeotropic alignment to produce the reorientation of field induced director axis.

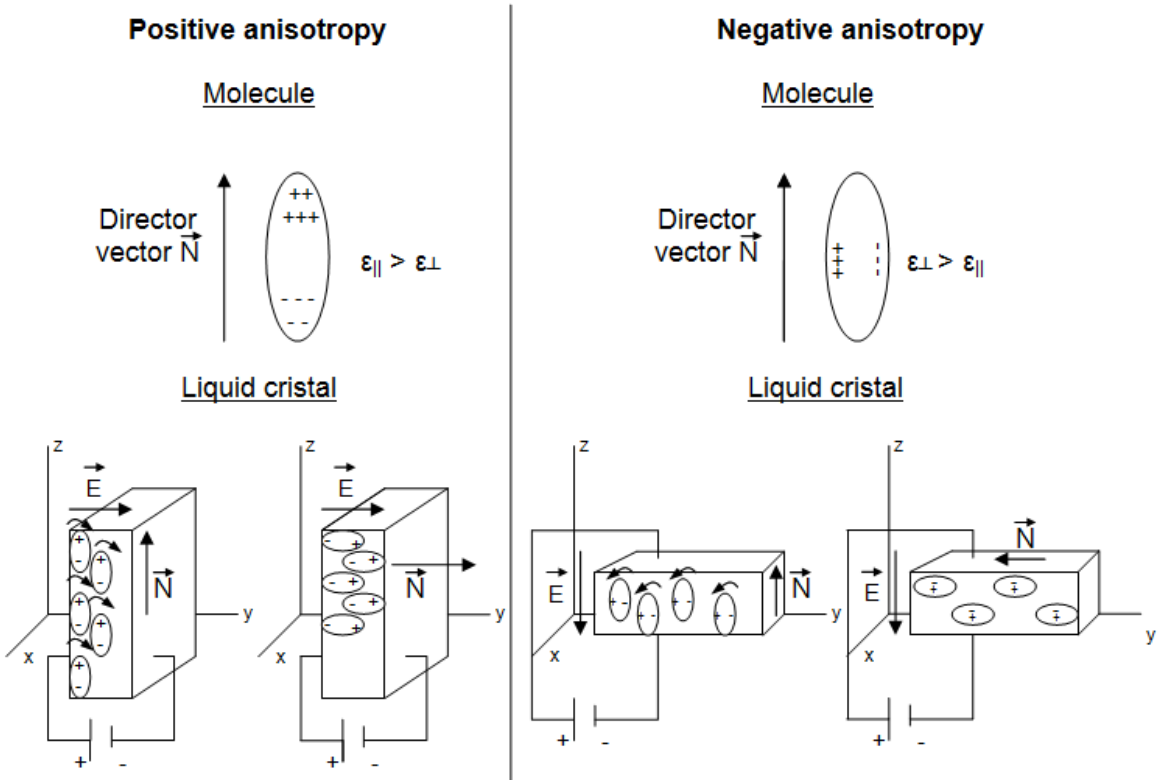

Figure 1.8: *Effect of an electric applied field on a nematic liquid crystal with planar alignment (left) and homeotropic alignment (right) that induces the reorientation of the director axis.*

After inducing the reorientation of the director axis with an ac field applied, the polarized light traversing the nematic cell experiences refractive index changes and phase shifts.

1.10 Objectives of the work

We have seen the main principles of VCSELs and nematic liquid crystals. Now, we will describe the objectives of this diploma work.

Nowadays, due to their low cost, small size and facility to be driven using conventional low voltage power suppliers, semiconductor lasers have become a broadly used coherent light source in our life. There is an increasing interest in using VCSELs as micro optic devices in various applications. However, their undefined polarization is a disadvantage.

The goal of this diploma work is investigate experimentally the impact of liquid crystal layer on the characteristics of vertical cavity surface emitting lasers. To this aim, we will use an experimental setup fully atomized and steered using Labview software and perform extensive investigation of the optical feedback from extremely short external cavity by measuring the characteristics of VCSELs behaviour such as spectral properties, total power emitted and polarization behaviour.

Finally, we will investigate experimentally the impact of filling in the ESEC by a nematic liquid crystal. We will investigate polarization resolved light versus distance characteristics, optical spectrum and polarization behaviour. We are especially interested in polarization and spectral properties because it is the first step to know if a liquid crystal overlay can be used for tuning the lasing properties of the VCSEL.

Chapter 2

Experimental results using the VCSEL and fiber

2.1 VCSEL characteristics

Fig. 2.1 shows the schematic setup used to characterize the solitary VCSEL.

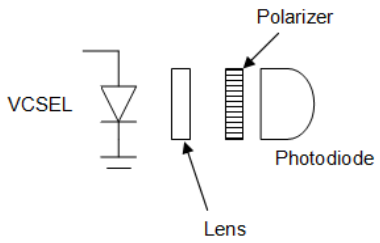

Figure 2.1: *Schematic setup used to measure the solitary case.*

The VCSEL is biased by a laser diode driver (LDD), which is a DC current source. We have used the module ITC-8022 of the Profile 8000 Modular Laser Diode Controller with 8 slots.

The VCSEL package is fixed in a holder by means of two screws. The holder has a 10kΩ thermistor temperature sensor and a Peltier cooling element attached to it with a thermal-conducting glue. We have used a temperature module controller (TED-8040) mounted inside the same modular controller as the LDD for measuring the temperature of the laser holder. The temperature is controlled by measuring the thermistor's impedance. The temperature electrically controller can set the temperature of the holder controlling the voltage applied to the Peltier element. It works in the range from 15 to 80ºC with an accuracy of ±0.01ºC. We have used a temperature of 25ºC with a fluctuation smaller than 0.01ºC. We use a VCSEL emitting at 850 nm.

The photodiode used is model 818-SL connected to a dual channel power meter, model 2832-C from Newport. The optical spectrum analyzer used is an AQ6317B from Ando Electric CO. It has a minimum wavelength resolution of 0.01nm.

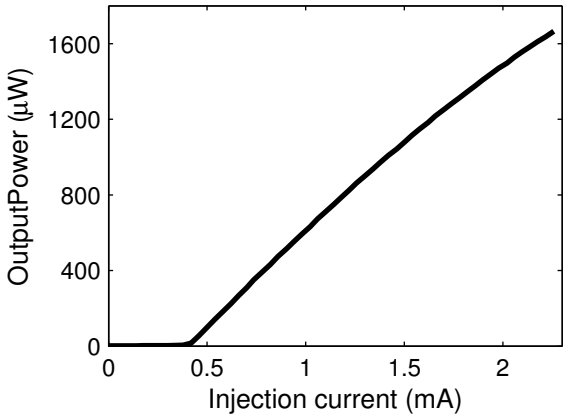

Figure 2.2: *Optical power versus injection current in the solitary case of the VCSEL.*

Fig. 2.2 shows the power versus current curve for the VCSEL. We place a polarizer between the VCSEL and the photodetector to obtain the polarization resolved output power versus injection current curve. We observe that there is not polarization switching between the two orthogonal linearly polarized modes when the injection current is varying – see Fig. 2.3.

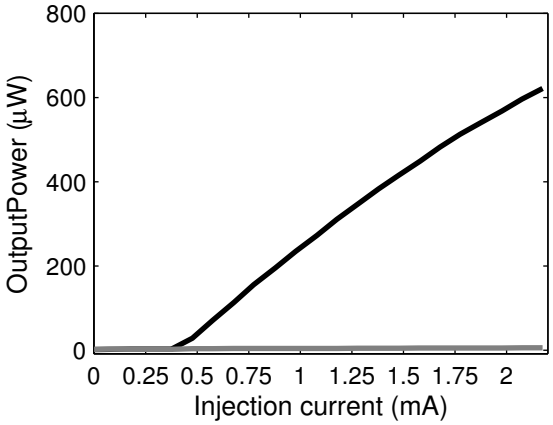

Figure 2.3: *Polarization resolved output versus injection current curve.*

2.2 Effects of feedback on the VCSEL. Experimental set-up

We want to analyze experimentally the effect of the feedback from an extremely short external cavity on the VCSEL. We need to create the short external cavity, so we use

a multimode fiber to carry out the rest of the experiments. The external cavity will be the air space between the VCSEL and the fiber.

Fig. 2.4 shows the schematic representation of the experimental setup and Fig. 2.5 and 2.6 show pictures of parts of it. The fiber is used to direct the light emitted by the VCSEL to the output. The fiber holder is mounted on a translation stage with 5 axis of freedom to get a precise alignment. The length of the cavity is varied by the movement of a DC step motor along the light emission direction of the VCSEL. The fiber is mounted on the motor. A microscope is used to determine the length of the cavity and to get a perfect alignment between the VCSEL and the fiber. There is less than 2 mm of fiber going out from the fiber holder to avoid vibrations or bending when the motor moves. We need to align properly the fiber in order to obtain the maximum output power at the end of the fiber. It is also necessary to keep a strong feedback.

The DC step motor is model M-111.DG (Physik Instrumente). It has a range of movement of 1.5 cm. The fiber is fixed on the movable part by a metallic holder and a cylindric fiber holder. The fiber holder is fixed between the two pieces of the matellic holder that has a circular groove – see Fig 2.5 and 2.6.

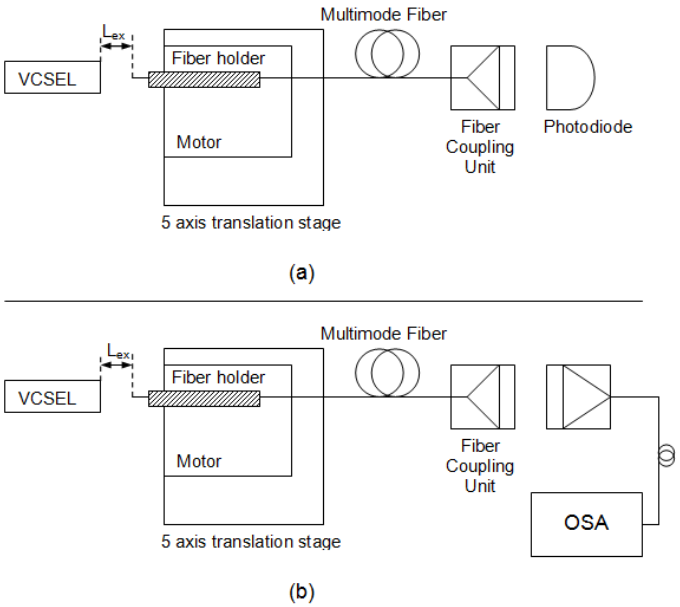

Figure 2.3: *Schematic representation of the experimental setup. (a) Setup used to measure PI curves and polarization resolved optical power for different lengths of the ESEC. (b) Setup used to measure the spectrum of light.*

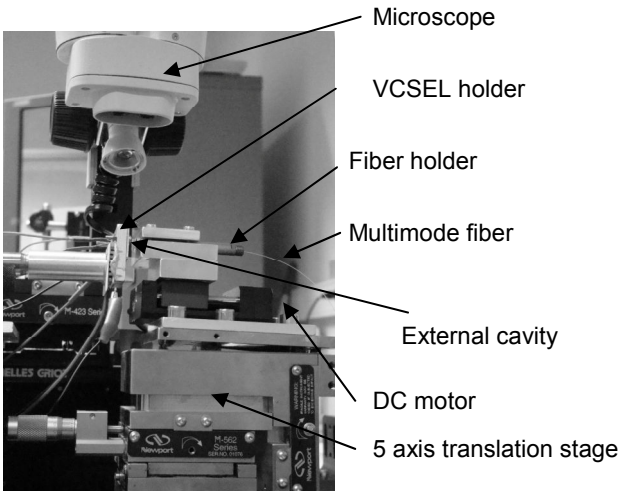

Figure 2.5: *Picture of the setup that shows how the fiber is used to create the extremely short external cavity*.

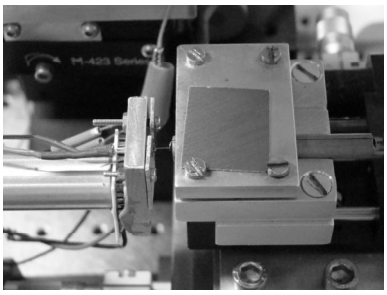

Figure 2.6: *Picture of the setup that shows how the light is coupled into the fiber*.

We can vary the external cavity length and the driving current of the laser. We are also able to measure the spectrum with an optical spectrum analyzer. For this purpose, it is necessary to replace one of the photodiodes with a fiber coupling unit that couples the light in another fiber. That fiber brings the light to the OSA – see Fig. 2.4 (b).

The motor, the laser driver, the power meter and the OSA can be controlled with a Labview program. With this program it is possible to sweep the length of the cavity and the current, measuring the output power and optical spectrum.

2.3 Impact of optical feedback on the VCSEL total power

In order to see the effect of optical feedback from an extremely short external cavity, we measure the optical power versus the external cavity length for a fixed current.

Initially, we place the fiber some millimeters far away from the VCSEL. Then, we move it towards the laser looking at the microscope to be sure that we do not hit the VCSEL. We know that the shortest distance at which we place the fiber is less than 25 μm. This value will be our relative zero.

We fix the injection current to 2 mA and sweep the length of the cavity in steps of 20 nm. The motor moves towards the laser. In Fig. 2.7 we show the optical power obtained.

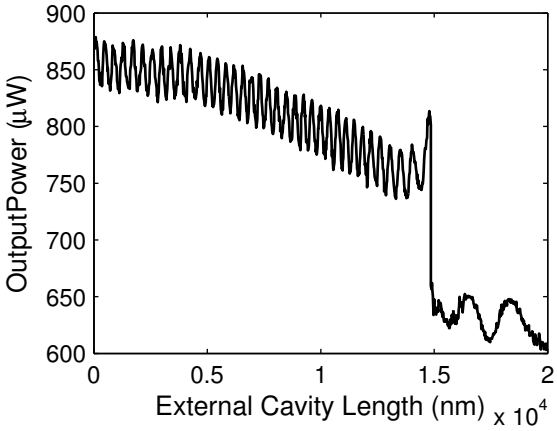

Figure 2.7: *Optical power when varying the EC length in a wide range.*

We can see the effect of the backlash of the motor. It needs some time to have enough inertia to move properly in steps of 20 nm. That is the reason why we do not observe the same sinusoidal modulation of the power the first 50 μm (right side of the figure) as when the fiber is near the VCSEL (left side of the figure).

Fig. 2.8 shows the power versus external cavity length. The cleaved facet of the multimode fiber works as an external mirror of 4% reflectivity. We observe the modulation of the output power with a period of half of the wavelength. It is also possible to appreciate that the output power decreases when the cavity becomes longer.

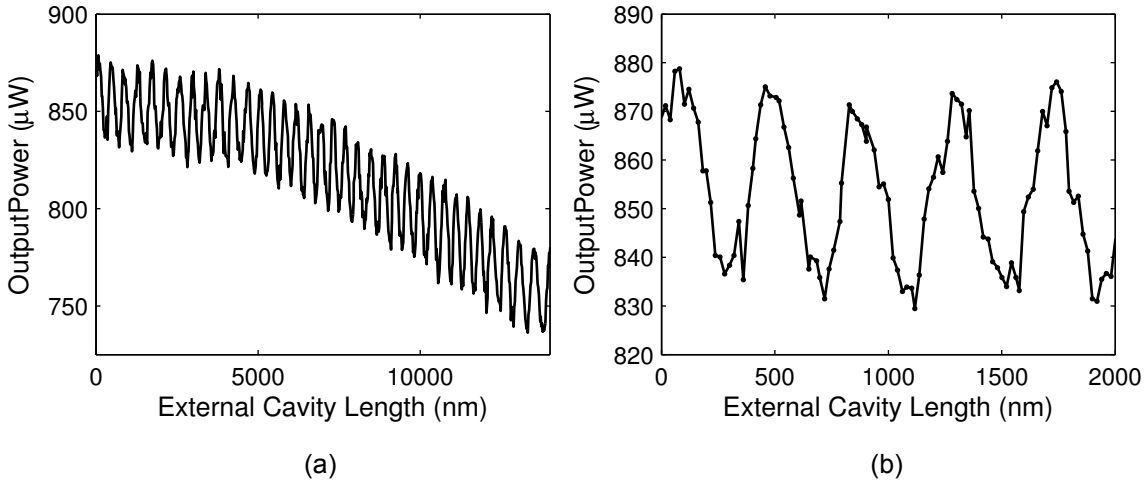

Figure 2.8: *(a) Optical power obtained varying the EC for a fixed current of 2 mA. (b) Expanded view.*

2.4 Impact of optical feedback on the VCSEL wavelength of operation

We measure the wavelength of operation versus the injection current curve at different fixed distances. We can see that the operation wavelength shifts with injection current. As shown in the Fig. 2.9, the slope of the curves is the same although we change the distance.

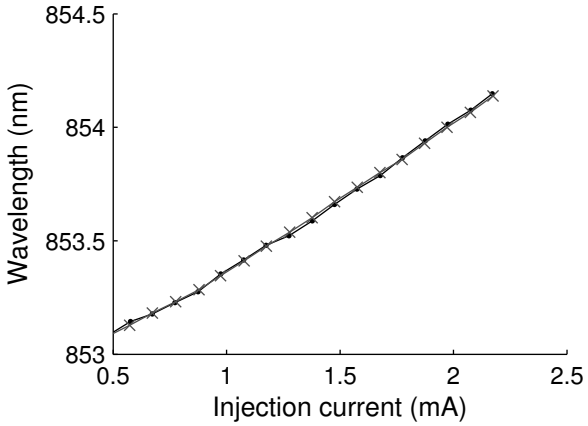

Figure 2.9: *Wavelength of operation of the laser versus current at two different lengths of the cavity: 0 nm and 12000 nm.*

We also observe the optical spectrum at two different fixed lengths of the cavity for different values of the injection current – see Fig. 2.10.

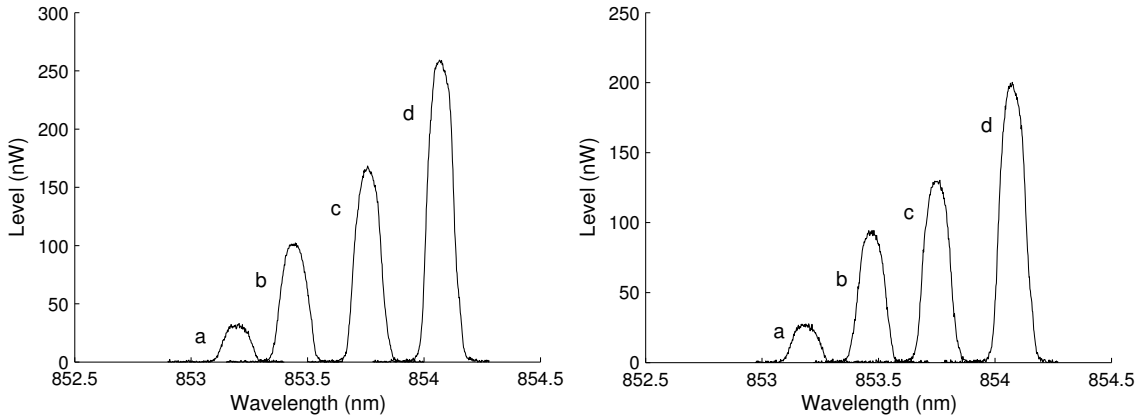

Figure 2.10: *Optical spectrum for distances of 0 nm (1) and at 12000 nm (2) at currents of 0.5 mA (a), 1 mA (b), 2 mA (c) and 2.5 mA (d).*

We carry out the experiment with the multimode fiber measuring with the OSA while the motor is moving (sweeping the cavity length). We observe the modulation of the wavelength of operation of the laser when the distance of the fiber changes (cavity length is varying). Fig. 2.11 shows the wavelength of light emitted versus the external cavity length.

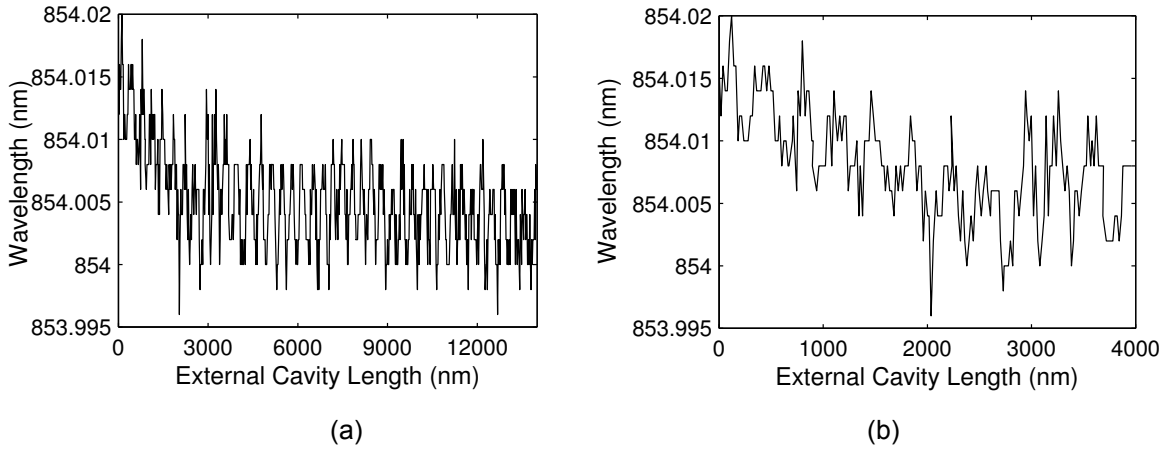

Figure 2.11: *Wavelength of light emitted versus EC length. (a) Wide range. (b) Small range.*

The wavelength modulation amplitude is very small and, due to the resolution of the OSA, it is not possible to see variations smaller than 0.01 nm. Therefore, there is not any appreciable increment or decrement on the amplitude. Performing longer sweeps of the length, the power coupled into the fiber is less than the minimum power sensitivity of the optical spectrum analyzer so we can not appreciate if the power is decreased.

Fig. 2.12 shows an external cavity length sweep at a fixed injection current of 2 mA. Both the total power and the wavelength are periodically modulated with a period of half of the wavelength of operation.

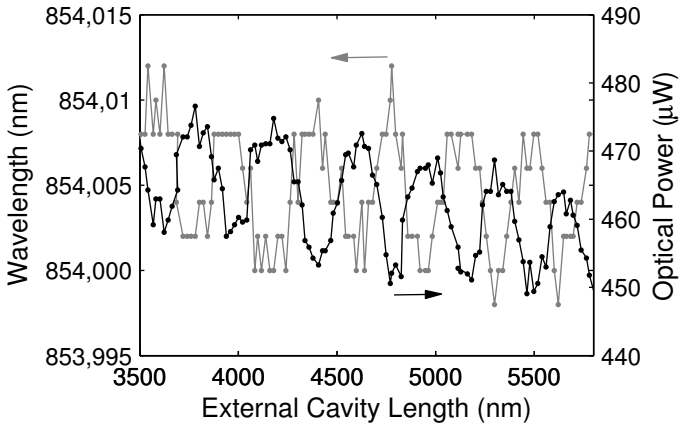

Figure 2.12: *Wavelength (grey line) and total power of the VCSEL (black line) as a function of the external cavity length for a fixed current of 2 mA.*

2.5 Impact of optical feedback on the VCSEL polarization properties

In order to see the effect of optical feedback from an extremely short external cavity on the polarization properties, we use a different setup – see Fig. 2.13.

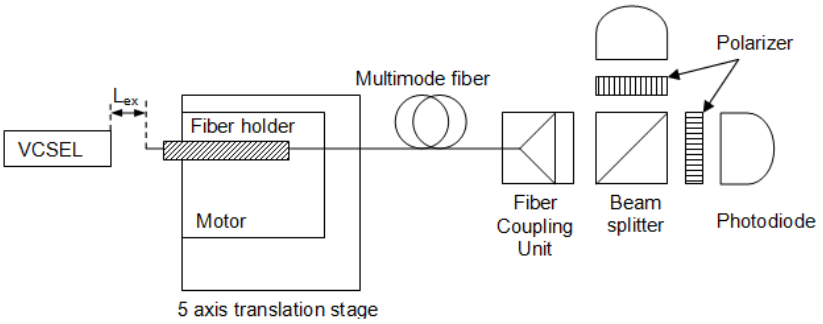

Figure 2.13: *Schematic representation of the experimental setup used.*

We place a non-polarizer beam splitter at the output. The reflected beam and the direct one go to two photodiodes through two polarizers. One polarizer selects one linear polarization mode and the other one selects the orthogonal mode. Both polarization modes are measured, so it is possible to obtain the polarization resolved optical power versus the injection current – see Fig. 2.14.

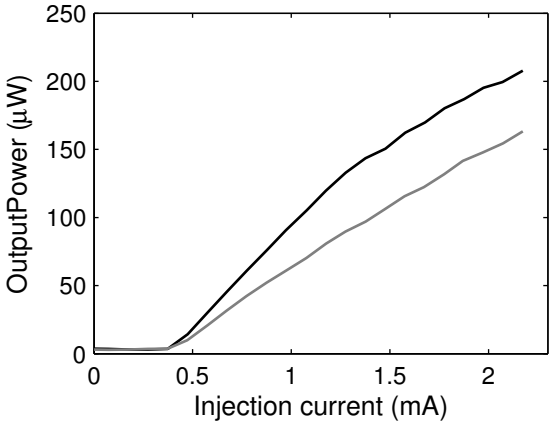

Figure 2.14: *Polarization resolved output power versus current using a long piece of multimode fiber. The two orthogonal linear polarization modes are represented in grey and black.*

The fiber that we use is a multimode one that does not maintain the polarization. If we use a long piece with bending or pressure on any point of it, it will introduce birefringence and the polarization at the end will not be linear.

In order to avoid this, we use a very short and straight piece of the multimode fiber to run the same experiment. The setup is the same as before, we only replace the fiber with another, shorter one. Doing this, we expect to have the polarization resolved power very similar to the one in front of the fiber. In Fig. 2.15, we show the polarization resolved power that we measure using the short piece of multimode fiber.

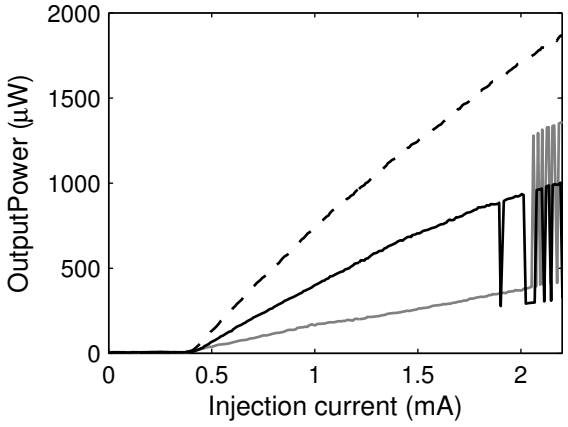

Figure 2.15: *Polarization resolved output power versus current using a short and straight piece of multimode fiber. Grey and black lines represent both LP modes. Dashed line represents total power.*

The minimum of the power is not zero for any of the linearly polarized modes, so the light going out of the fiber is elliptically polarized, not linear. The fiber introduces a birefringence that changes the polarization from linear at the input to elliptical at the output. The birefringence could be a consequence of the stress applied to the fiber in the holders. However, the fiber stress-induced birefringence does not prevent if there is polarization switching. We can observe behaviour around 2 mA which resembles polarization switching, however this has not been reproduced in the consecutive experiments.

To be sure that there is polarization switching, we change the length of the cavity for fixed values of current near 2 mA. We do not appreciate the polarization switching. One of the polarization modes has more power than the other for all the values of the ESEC length, as it is shown in Fig. 2.16.

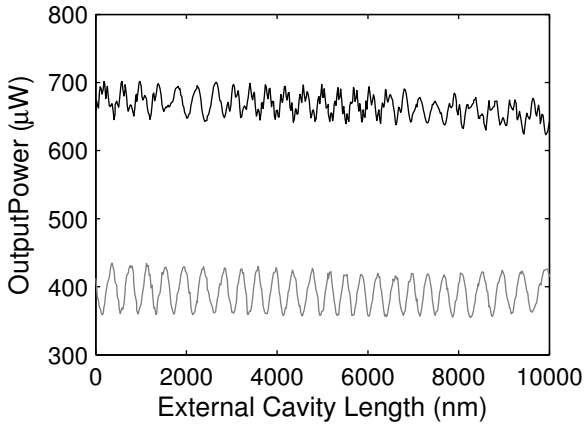

Figure 2.16: *Polarization resolved output power as a function of the external cavity length for a current of 1.8 mA. Grey and black lines represent both LP modes.*

After a problem with the fiber, we replace it. We put again a short and very straight piece of multimode fiber to perform the experiment. Fig. 2.17 shows the polarization resolved power versus injection current measured.

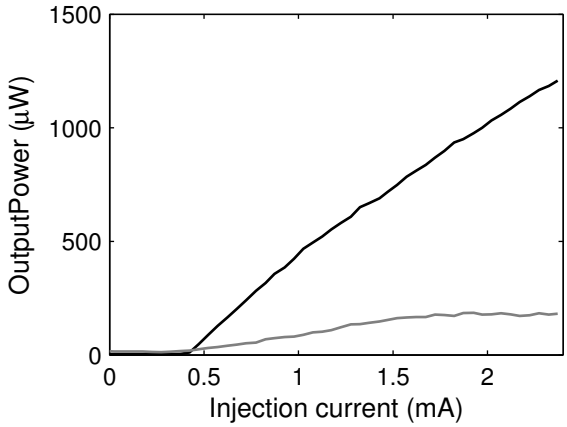

Figure 2.17: *Polarization resolved output power versus current using the new short piece of multimode fiber. Grey and black lines represent both LP modes.*

We can not see any switching as we did before. We also can see that the power of one of the modes is almost zero. A priori, the index of refractivity of both fibers is more or less the same, so the reflectivity of the external cavity should be the same. As a consequence, the change of the polarization does not depend on the fiber replacing. The distance or the angle between the fiber and the VCSEL may have changed. Perhaps, the switching in the previous experiment was a consequence of the optical feedback from the far end of the optical fiber and not from the feedback of the ESEC.

We try to align the fiber better and to place it closer. We also cut again the fiber and clean the cleaved facet to be sure that there are not impurities on it. We get more power but we do not see any change in the polarization. In fact, we lose that minimum we had for one of the LP modes – see Fig. 2.18.

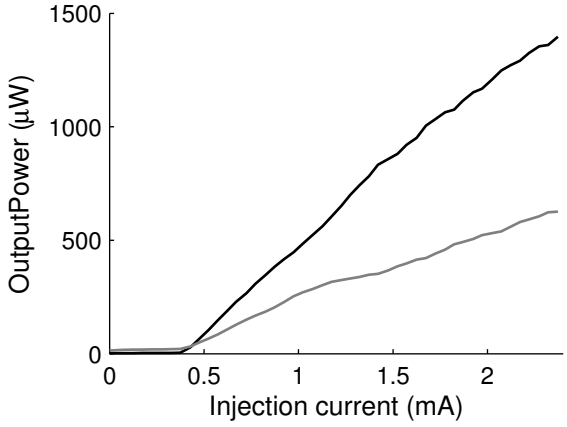

Figure 2.18: *Polarization resolved output power versus current changing the alignment. Grey and black lines represent both LP modes.*

Fig. 2.19 shows the polarization resolved power versus the external cavity length. We do not appreciate any switching. There is one mode with more power than the other one for all the current values while varying the length of the cavity.

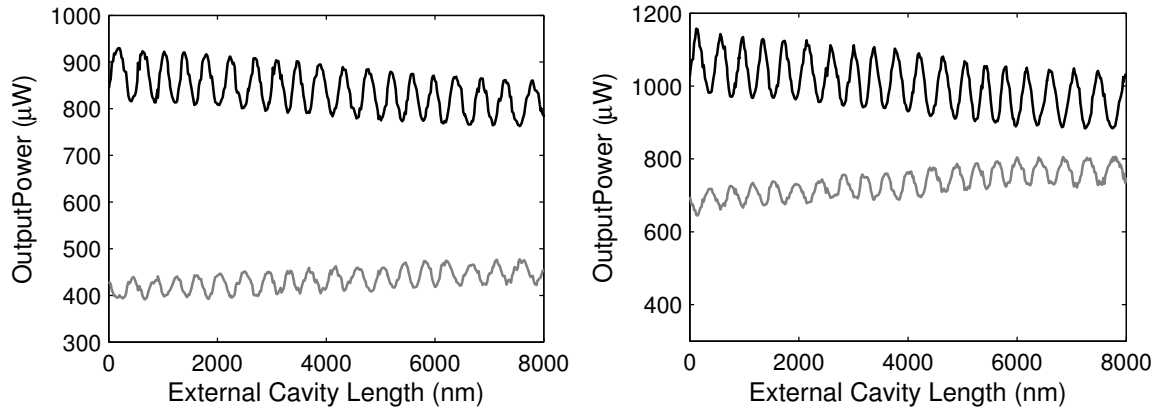

Figure 2.19: *Polarization resolved output power as a function of the ESEC length for a fixed current of 1.5 mA (a) and 2 mA (b). Grey and black lines represent the two LP modes.*

2.6 Gluing metallic mirrors

We use the cleaved facet of the multimode fiber as a mirror but the reflectivity is low, so we use an external mirror glued on the cleaved facet. The fiber holds the mirror and guides the light to the output.

Fig. 2.20 shows pictures of the setup used. First of all, we put the optical fiber with a perpendicularly cleaved facet on a fiber holder. That fiber holder is placed on a plastic piece held to another piece to create one right angle. We hold this to a vertical translation stage to allow us to precisely move down and up the facet of the fiber. The glass with the metallic layer that we use as a mirror is fixed by means of one screw and a metallic plate to a two axis translation stage. That translation stage allows us to select the exact position of the metallic layer where we are going to glue the fiber. The cleaved facet of the fiber is perpendicular to the mirror. Then, we deposit carefully a tiny drop of ultra violet curing on the fiber facet. When the glue is dried, the refractive index of it is the same as the one of the fiber for preventing unintentional reflectivities from the interface between the glue and

the fiber. The drop of glue is very small, so its diameter is approximately same size than the fiber one. Using the vertical translation stage, we move the fiber facet with the drop of glue toward the metallic mirror until the glue touches it. We observe with an objective when the drop of glue stops having a round shape. At this moment, the glue is touching the mirror.

We dry it using a UV light source for 30 minutes to be sure that it is perfectly glued. After that, we pull a little bit from the fiber by means of the vertical translation stage. Next, we scratch with a needle on the mirror surface at the limit of the dried glue causing the mirror to break just from the border of the glue.

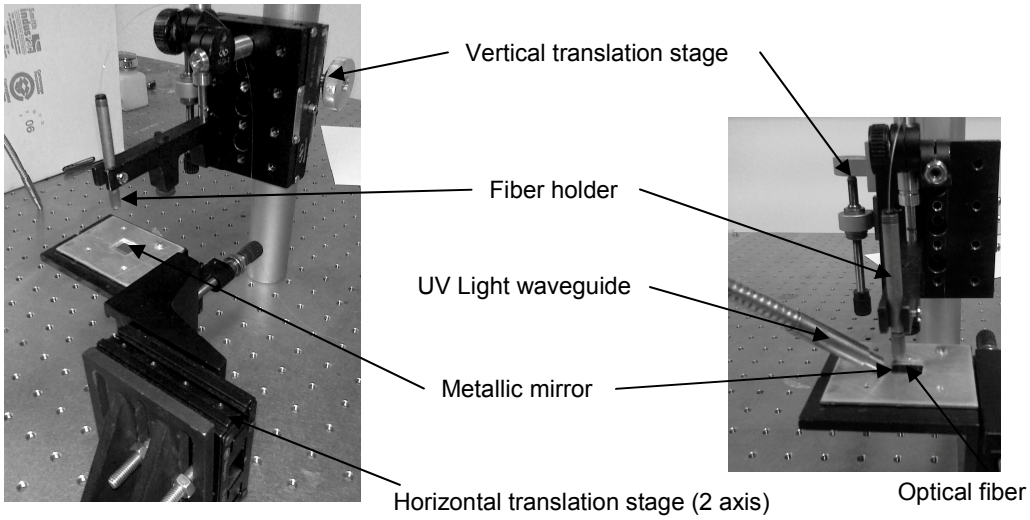

Figure 2.20: *Setup used for gluing the metallic mirrors.*

We have three different metallic mirrors. In order to know the approximate value of reflectivity of them, we use a small setup. The light emitted by the laser goes directly to a photodiode connected to the powermeter. There is a distance between the VCSEL and the photodetector. Each mirror is fixed on a holder that we put between the VCSEL and the photodetector. The output power is measured and compared to the one that we have without putting any mirror. The beam that goes out of the laser is divergent, so we can put a lens before the mirror to collimate the light. However, the results of power measured are very similar and do not change the values of the reflectivity that we get.

	Power (μW)	Reflectivity
No mirror	975	-
Mirror 1	112	88 %
Mirror 2	72	93 %
Mirror 3	125	87 %
Mirror 4	40	96 %

The values of the different reflectivities are similar and therefore, we decide to work with only mirror in all the experiments. It is the one with R = 88 %.

2.7 Impact of stronger optical feedback on VCSEL properties

We perform the same experiment with a mirror glued to the cleaved multimode fiber facet. In Fig. 2.21 we show the optical power when varying the length of the cavity. We can observe that the amplitude of the output power modulation is bigger with the mirror than without it due to the stronger feedback that we have now.

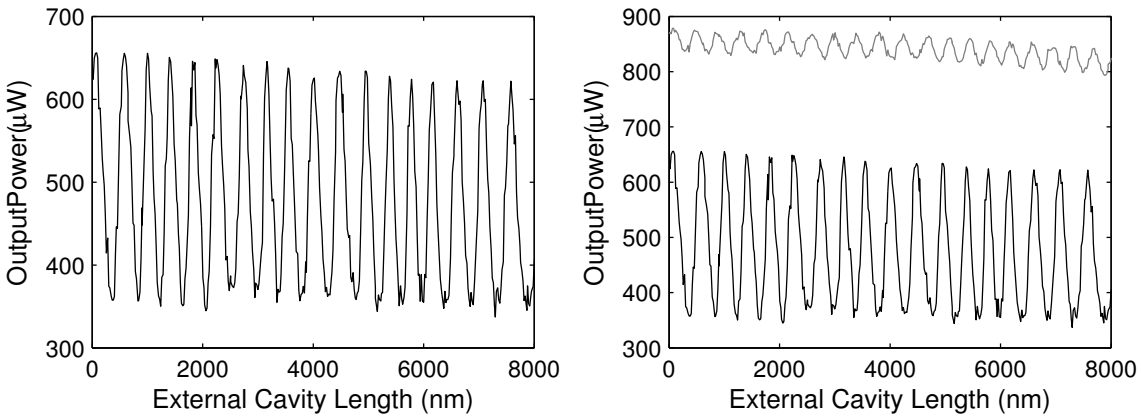

Figure 2.21: *(a) Optical power obtained varying the EC length for a fixed current of 2 mA using multimode fiber with a mirror. (b) Power modulation using multimode fiber with a mirror (black, lower trace) and without mirror (grey, upper trace).*

In Fig. 2.22 we show the polarization resolved power using multimode fiber with mirror. We can not observe the polarization switching between the two orthogonal linearly polarized modes when the injection current is varying. As in the case of multimode fiber

without mirror, this might be because the small piece of multimode fiber that we are using is introducing a birefringence in the fiber that changes the polarization. So, we observe that both modes of polarization have similar values of power in the whole range of injection current. There is not a considerable difference between the power values of the different polarization modes because due to the birefringence, the polarization observed at the output is not linear. It has changed to almost circular polarization.

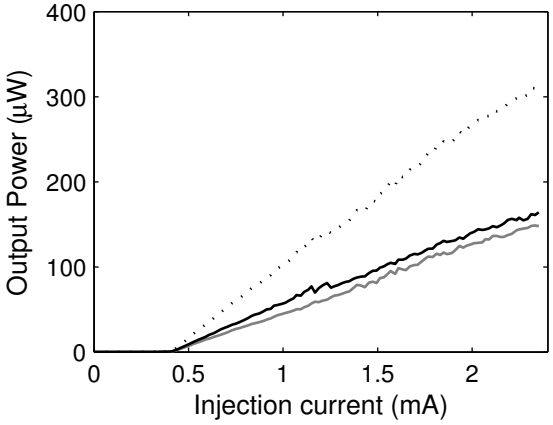

Figure 2.22: *Polarization resolved output power versus current using multimode fiber with mirror. Grey and black lines represent both LP modes. Dashed line represents total power.*

We want to have linear polarization at the end, so what we can do is to introduce a new birefringence in the fiber applying pressure or stress to one point of the fiber to separate perfectly the two linear polarization modes.

Before introducing a new birefringence, we realise that we have a new problem. We observe many peaks in the curves of output power. It seems like noise. We have the fiber and the VCSEL very well fixed, as the rest of the setup components. We work with a pressurized optical table that makes the setup very stable. However, we see some randomly variations on the signal – see Fig. 2.23.

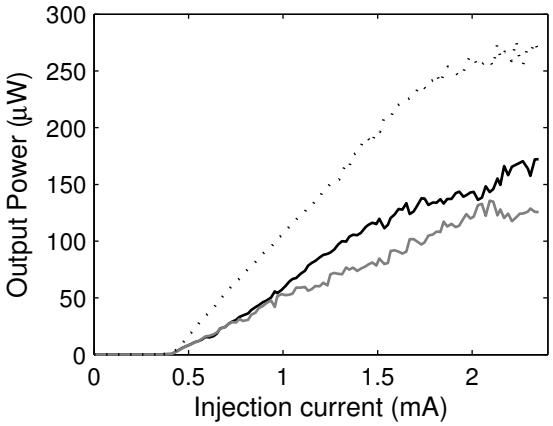

Figure 2.23: *Polarization resolved output power versus current. Grey and black lines represent both LP modes. Dashed line represents total power. There is some noise on the signal.*

Trying to find out why we have that noise, we perform the experiment without people in the lab, biasing the laser at a constant temperature and driving current – see Fig. 2.24.

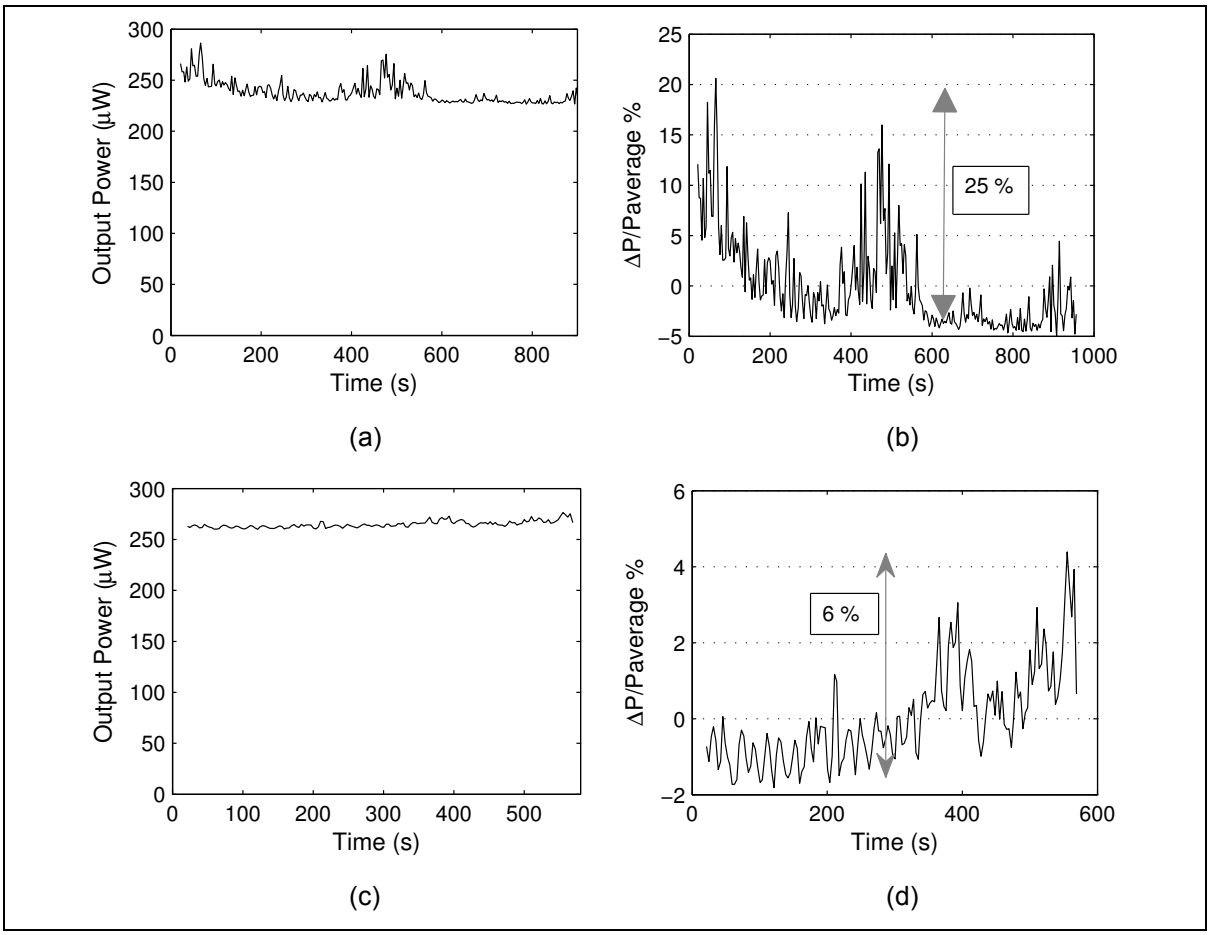

Figure 2.24: *Optical power emitted during non-laboratory hours. Absolute (a)(c) and relative (b)(d) variations of the power.*

As it is shown in the Fig. 2.24, we have different values of noise at the same conditions. Something is not stable in the setup.

The problem could be the contact between the mirror and the wires of the VCSEL that can originate some vibrations in the edge of the fiber. In Fig. 2.25 we show a schematic of that contact. We need to put the fiber close to the VCSEL to create the extremely short external cavity and this laser has very long wires, so they are touching during the running of the experiment and the angle of the fiber can change a little.

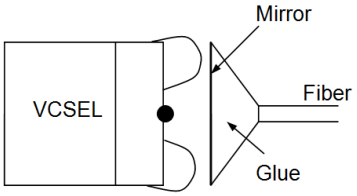

Figure 2.25: *Schematic of the contact between the wires of the VCSEL and the mirror glued to the fiber.*

We repeat everything with a smaller mirror in order to minimize the contact but the results are quite similar. Finally, we find that the problem was one of the photodetectors that did not work properly. We replace it and continue with the experiments.

We run the experiment with another photodiode and the short piece of multimode fiber with a mirror glued and we realise that there is a physical phenomenon occurring. We see a modulation in the PI curve – see Fig. 2.26.

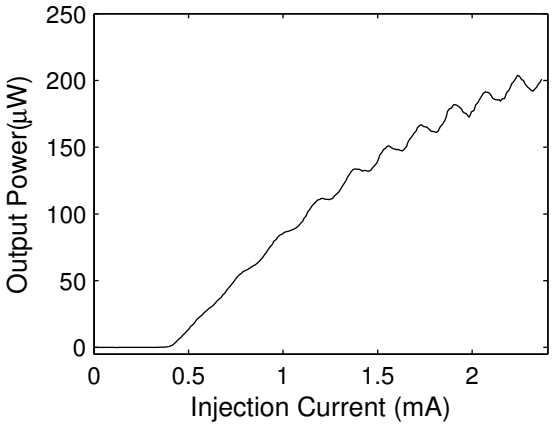

Figure 2.26: *Total output power versus current injection current.*

The modulation of the output power with injection current is due to the wavelength shift caused by the current self-heating of the VCSEL.

Fig. 2.27 shows the total power measured when varying the length of the cavity for a fixed injection current of 2 mA using a short piece of multimode fiber after replacing the photodiode.

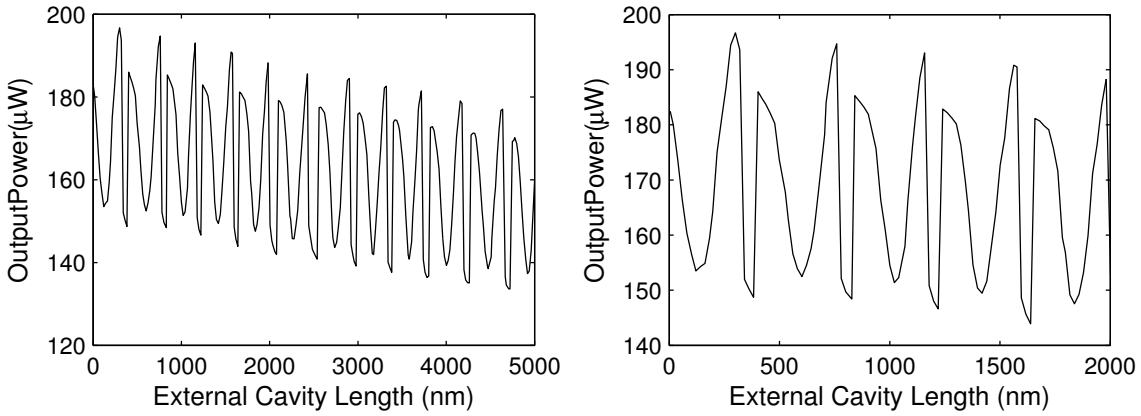

Figure 2.27: *(a) Total optical power obtained varying the EC for a fixed current of 2 mA using the multimode fiber. (b) Zoom.*

We expect to observe a modulation of the output power with a period of half of the wavelength as before. However, we see a modulation that is not perfectly sinusoidal. The power is increasing (drawing the sinusoid) and when arrives to the maximum, it goes down suddenly and then it goes up and continues drawing the sinusoidal wave. We explain this to be due to polarization switch and different losses for each polarization mode, so that the total output power changes, too.

Using a mirror, the reflectivity has increased and polarization switching can appear. We place a polarizer at the end of the fiber to see if the power decreases to zero at these points. In Fig. 2.28 we show the polarization resolved power of one linear polarization mode versus the external cavity length.

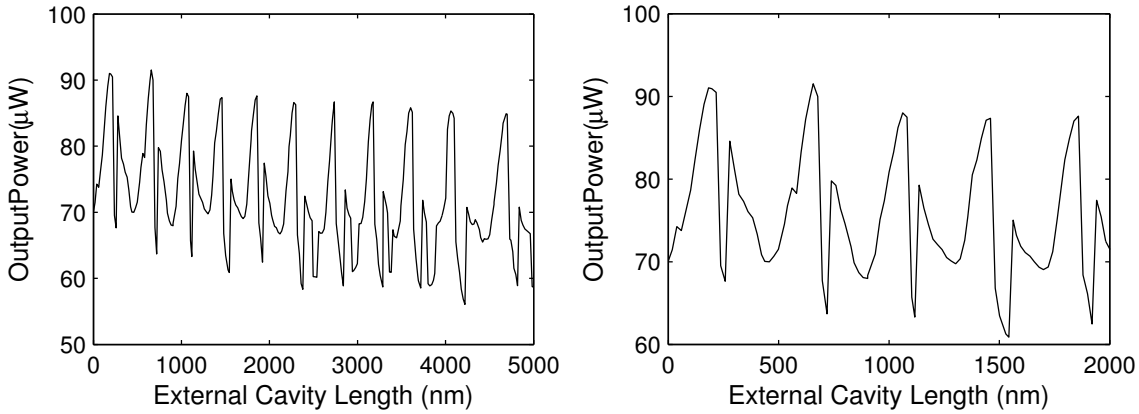

Figure 2.28: *(a) Polarization resolved optical power of one LP mode obtained varying the EC for a fixed current of 2 mA using the multimode fiber. (b) Zoom.*

We see that the value of the power of one polarization mode decreases at those points, but it is not zero. This is due to the not perfect linear polarization because of the birefringence introduced by the multimode fiber.

Fig. 2.29 shows the light spectrum at a fixed current of 2 mA for lengths of the extremely short external cavity of 0 nm and 2000 nm.

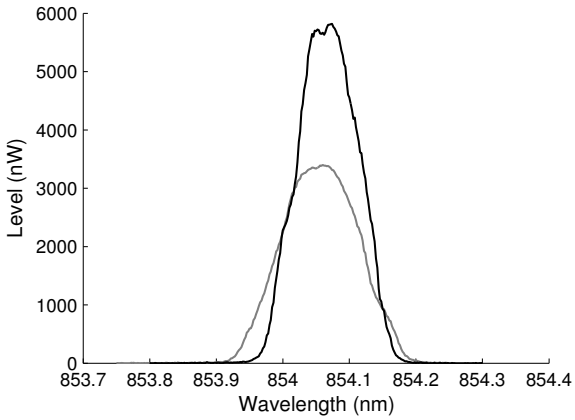

Figure 2.29: *Optical spectrum at the output at one fixed current of 2 mA for a cavity length of 0 nm (black) and 2000 nm (grey).*

2.8 Experimental results using fiber polarization controller

We use the same setup replacing the fiber with one longer to have space enough to place a polarization controller on the table. The controller is standard size in-line

polarization controller without fiber, model FPC-100 (OZ Optics). It allows one to convert any input polarization to any desired output polarization. It works by applying pressure with an adjustable clamp on the fiber that causes a birefringence within the fiber core. Changing the pressure varies the delay between the different polarization components. We try to use it in our setup, with the multimode fiber, but the pressure applied is not enough to introduce a birefringence so strong that separates the liner polarization modes. Therefore, we change the multimode fiber to a singlemode fiber that works at 850 nm.

It is very difficult to get a high value of power at the end using singlemode fiber because the core is very thin and it is difficult to do the coupling. That is the reason why we do not use any mirror glued to the fiber. If we put a mirror, the power detected at the output would be strongly influenced by the noise level of the photodetector.

Fig. 2.30 shows the polarization resolved power versus injection current using singlemode fiber.

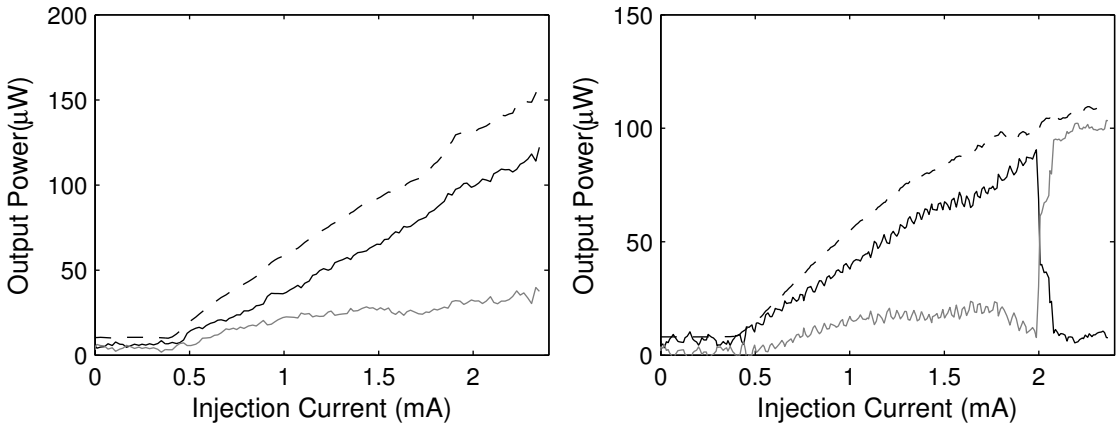

Figure 2.30: *Polarization resolved output power versus current using a single mode fiber at a distance of 0 nm. Grey and black lines represent both LP modes. Dashed line represents the total power. (a) Without switching. (b) Polarization switching at 2 mA.*

We can observe the polarization switching between the two orthogonal linearly polarized modes when varying the injection current (Fig. 2.28(b)). We can not see it all the times we run the experiment (Fig. 2.28(a)). It might be because of the high vibrations we have in the lab due to the preparations for the renovation in the department.

Trying to know what happens and if there is polarization switching, we sweep the length of the cavity for fixed values of current near 2 mA. In Fig. 2.31 it is shown the behaviour that we observe.

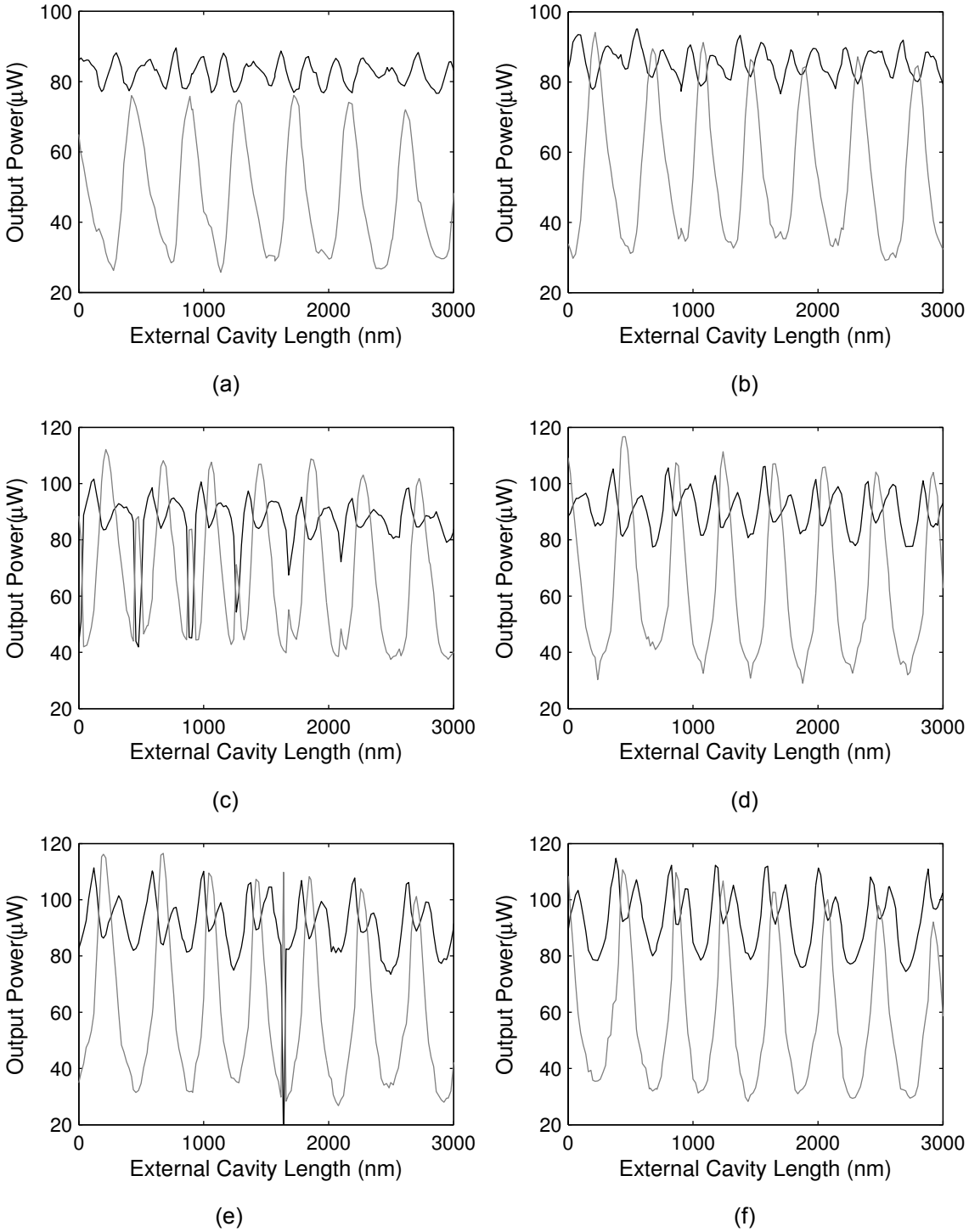

Figure 2.31: *Experimentally obtained polarization resolved optical power at fixed currents of: (a) 1.8 mA, (b) 1.9 mA, (c) 2 mA, (d) 2.1 mA, (e) 2.2 mA and (f) 2.3 mA.*

We see polarization switching in some points (Fig.2.30). However, these switchings are not persistent indicating that the polarization selection mechanism induced by extremely short external cavity is not strong enough. Fig. 2.32 shows an expanded view where it is possible to see the not persistent switchings.

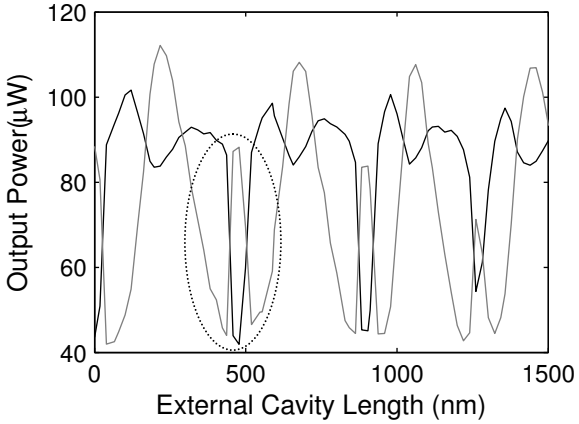

Figure 2.32: Zoom on the experimentally obtained polarization resolved optical power at a fixed current of 2 mA.

Chapter 3

Experimental results on VCSEL with optical feedback from extremely short external cavity containing a liquid crystal

3.1 Experimental setup

In order to see the impact of liquid crystal, we use the same setup as before with a short and straight piece of multimode fiber without mirror – see Fig. 3.1. The only difference is that we put a drop of liquid crystal on the pedestal of the VCSEL.

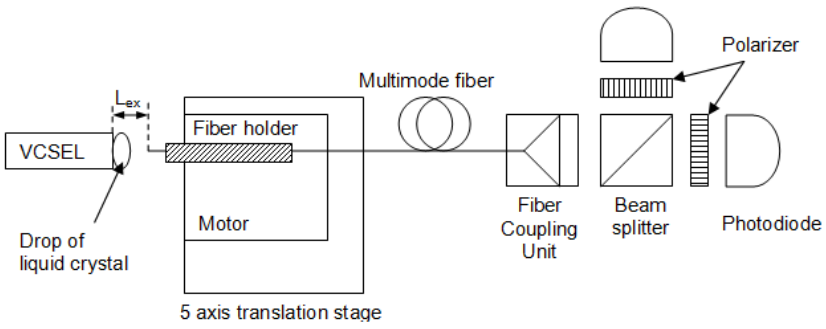

Figure 3.1: *Experimental setup used with the LC drop.*

The liquid crystal is nematic E7, with refractive indices $n_o = 1.51$ and $n_e = 1.71$. Looking with the microscope and using a plastic syringe, we put a drop on the pedestal of the VCSEL trying to not have any bubble of air. Then, we wait almost one hour to be sure that it loses the viscosity and becomes compact for remaining there. If we do not wait, it can flow like a normal liquid and fall over the pedestal.

3.2 Effect of the liquid crystal drop on the VCSEL characteristics

First, we measure the characteristics of the VCSEL directly, without the fiber and the rest of the setup, to see the effect of the liquid crystal. Placing something on the VCSEL, a new cavity is created and we want to observe its influence. Fig. 3.2 shows the optical power versus injection current of the VCSEL with the liquid crystal and in the solitary case of the VCSEL.

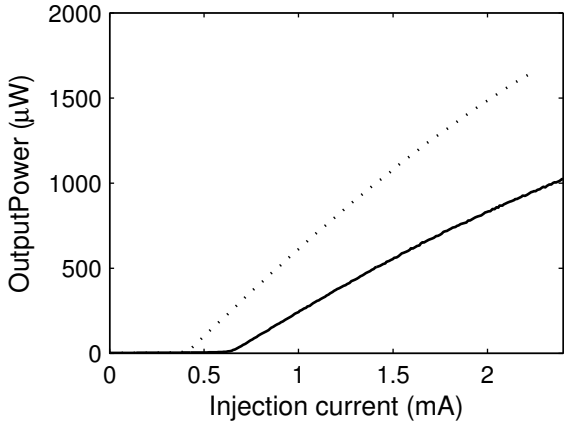

Figure 3.2: *Optical power versus injection current of the VCSEL with the drop (black line) and in the solitary case of the VCSEL (dashed line).*

The curve obtained with the LC drop is different from the one of the VCSEL solitary. The power is lower and it increases when the current is increasing with a smoother slope. We can see also that the threshold current is now higher than 0.5 mA and, in the solitary case of the VCSEL, it was smaller.

Fig. 3.3 shows the polarization resolved output versus injection current curve. Now, the polarization at the output of the liquid crystal is not linear. Varying the angle of the polarizer, we get the same power for all the values. Comparing Fig. 3.3 (a) and (b), we can see that the polarization resolved light versus current curves only slightly change when aligning the polarizer to the maximal power at different injection currents.

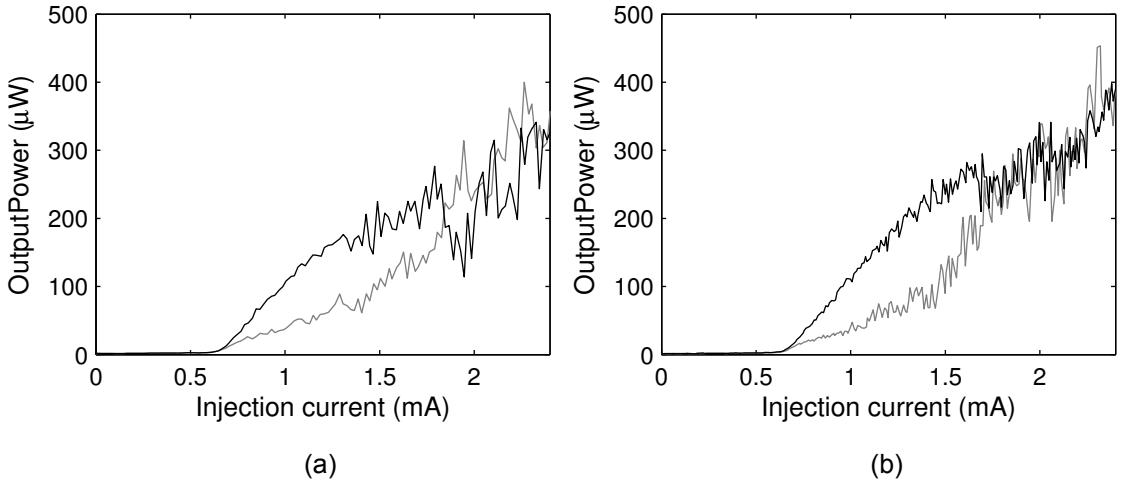

Figure 3.3: Polarization resolved output versus injection current curve. (a) Measured when there is a maximum on 1 mA. (b) Measured when there is a maximum on 2 mA.

3.3 VCSEL with optical feedback from extremely short external cavity containing nematic liquid crystal

We need to create a small cavity of liquid crystal between the VCSEL and the fiber. It is very difficult to align the fiber and put it close to the VCSEL because it enters in the drop of liquid crystal and we can not see with the microscope if it is exactly in front of the laser. When the fiber is moving towards the drop and touches it a bit, the drop distorts as it is entered by the fiber – see Fig. 3.4. If we continue moving the fiber, the drop recovers its original shape. L_{LC} is the extremely short external cavity length when filled in with liquid crystal.

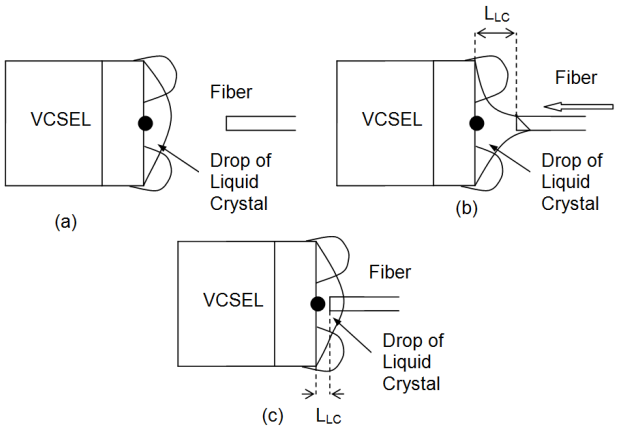

Figure 3.4: *Process of introducing the fiber into the liquid crystal drop.*

First, we fix the distance of the fiber at our relative zero and measure the polarization resolved output power versus current when using multimode optical fiber – see Fig. 3.5. Observing the case of the average, we can see that the powers of both polarization modes are almost the same.

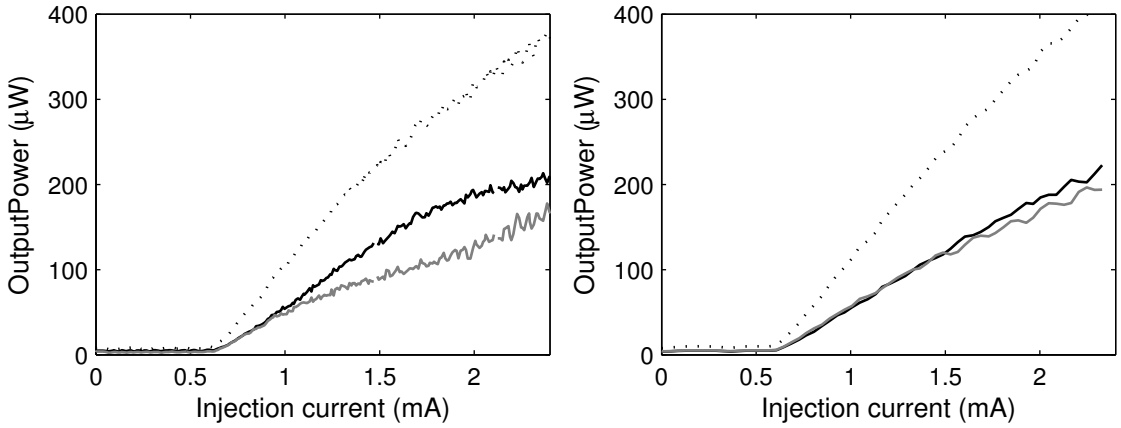

Figure 3.5: *Polarization resolved output power versus injection current with multimode fiber and the drop of LC. Grey and black lines represent both LP modes. Dashed lines represent total power. (a) One acquisition. (b) Average of 20 samples.*

Trying to find out what is the behaviour of the power as a function of time, we perform an experiment by biasing the laser at a constant temperature and driving current and measuring continuously the power of the two polarization modes – see Fig. 3.6.

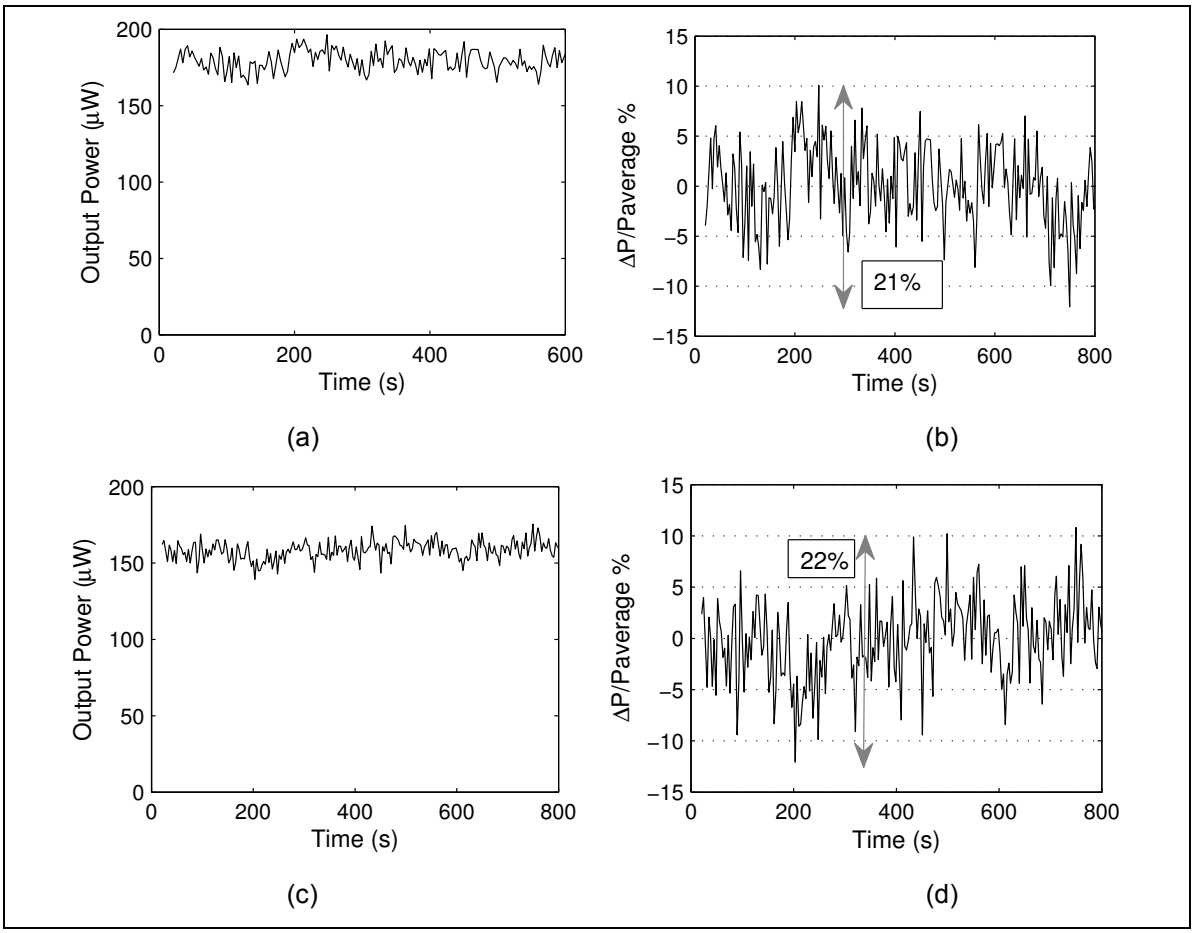

Figure 3.6: *Polarization resolved output power emitted. Absolute (a)(c) and relative (b)(d) variations of the power of each polarization mode.*

As can be seen, the power of one polarization mode (Fig. 3.6 (a)) varies randomly as a function of time with amplitude from 156 to 196 μW and standard deviation of 7.05 μW. The amplitude of power of the other polarization mode (Fig. 3.6 (b)) varies from 139 to 175 μW with a standard deviation of 6.24 μW.

We measure the light versus current curves for different distances from the VCSEL and we observe similarly the same behaviour – see Fig. 3.7.

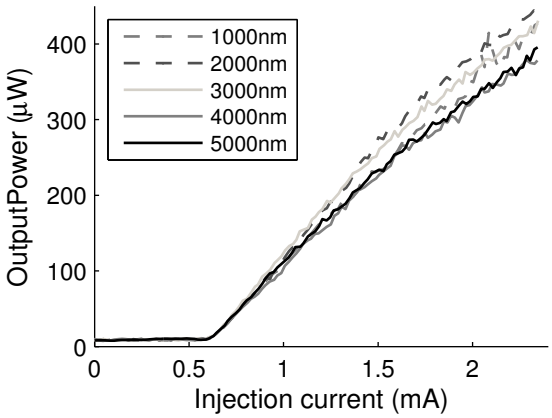

Figure 3.7: *Total optical power versus injection current for different lengths of the liquid crystal cavity.*

We use the OSA for measuring the optical spectrum at two different fixed lengths of the liquid crystal cavity for different values of the injection current – see Fig. 3.8. We get very low values of power. The optical spectrum at 0.5 mA is almost insignificant due to the small power we have.

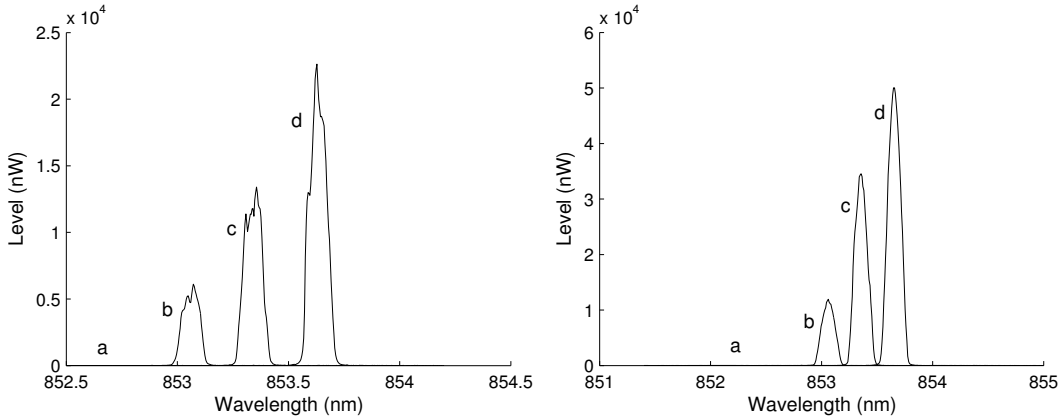

Figure 3.8: *Optical spectrum for distances of 0 nm (1) and at 2000 nm (2) at currents of 0.5 mA (a), 1 mA (b), 2 mA (c) and 2.5 mA (d).*

Fig. 3.9 shows the optical spectrum at fixed currents of 1.5 mA and 2 mA for two different distances. We can see that the spectral position of the emission light does not change for fixed currents when the length of the cavity is increased.

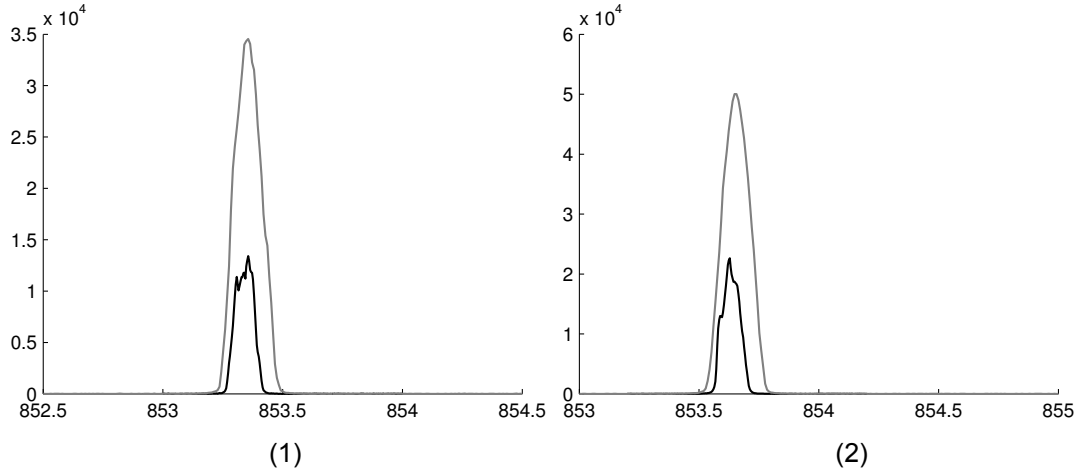

Figure 3.9: *Optical spectrum at fixed currents of 1.5 mA (1) and at 2 mA (2) for distances of 0 nm (grey line) and 2000 nm (black line).*

We fix the injection current to 1.8 mA, 1.9 mA, 2 mA, 2.1 mA and 2.2 mA, and perform the experiment of sweeping the length of the cavity in steps of 20 nm – see Fig. 3.10. The motor moves towards the laser. We obtain for all the values of current a very similar result. We can not see any effect or significant behaviour. This might be because the difficulties we have coupling the fiber. We place it closer to the VCSEL, so near that we can not appreciate with the microscope if there is a separation between the laser and the fiber. We repeat the experiment of moving the motor towards the VCSEL in steps of 20 nm and show the result in Fig. 3.11.

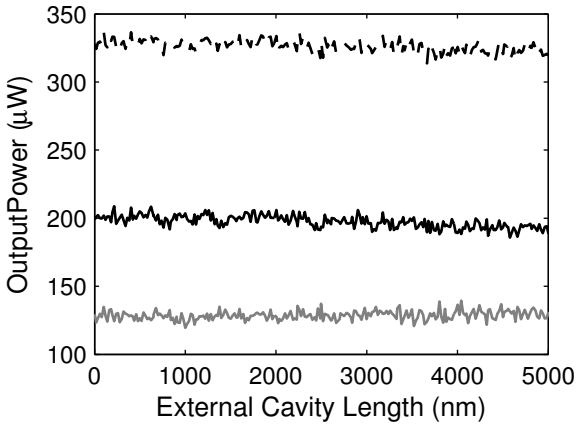

Figure 3.10: *Polarization resolved output power at different lengths of the LC cavity for a current of 2 mA. Grey and black lines represent the two LP modes. Dashed line represents the total power.*

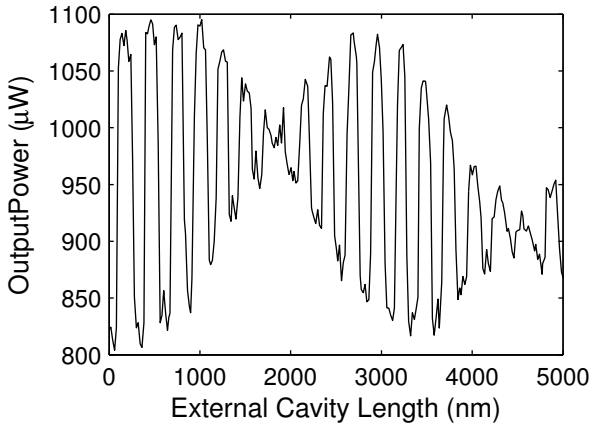

Figure 3.11: *Optical power obtained varying the LC cavity for a fixed current of 2 mA.*

We observe a double modulation of the power curve. The modulation of the output power with a period of P_1 = 300 nm has its amplitude modulated also with a period of P_2 = 10 · P_1. P_1 corresponds to half the optical path in the extremely short external cavity:

$$\frac{2\pi}{\lambda} n_{LC} \cdot L_{LC1} = m\pi$$

$$\frac{2\pi}{\lambda} n_{LC} \cdot L_{LC2} = (m+1) \cdot \pi$$

$$\frac{2}{\lambda} n_{LC} \cdot (L_{LC2} - L_{LC1}) = 1$$

$$P_1 = L_{LC2} - L_{LC1} = \frac{\lambda}{2n_{LC}}$$

where m is an integer that gives the interference order. From the last equation, we get:

$$300 = \frac{850/2}{2n_{LC}} \quad \Rightarrow \quad n_{LC} = \frac{425}{300} = 1.5$$

This corresponds to the ordinary refractive index n_o of the liquid crystal. In a similar way, the 10 cycle modulation will correspond to:

$$3000 = \frac{425}{\Delta n} \quad \Rightarrow \quad \Delta n = \frac{425}{3000} \approx 0.15$$

This is more or less equal to the liquid crystal birefringence: $\Delta n = n_e - n_o$.

We observe a modulation of the amplitude in the two polarization modes and a number of polarization switchings. However, in contrast to the case of VCSEL with isotropic extremely short external cavity [9], the polarization switches are not complete. In Fig. 3.12 we show the polarization resolved power as a function of the external cavity

length when filled in with liquid crystal. Fig. 3.13 shows an expanded view of Fig. 3.12 in the region of L_{LC} with values from 0 to 4000 nm.

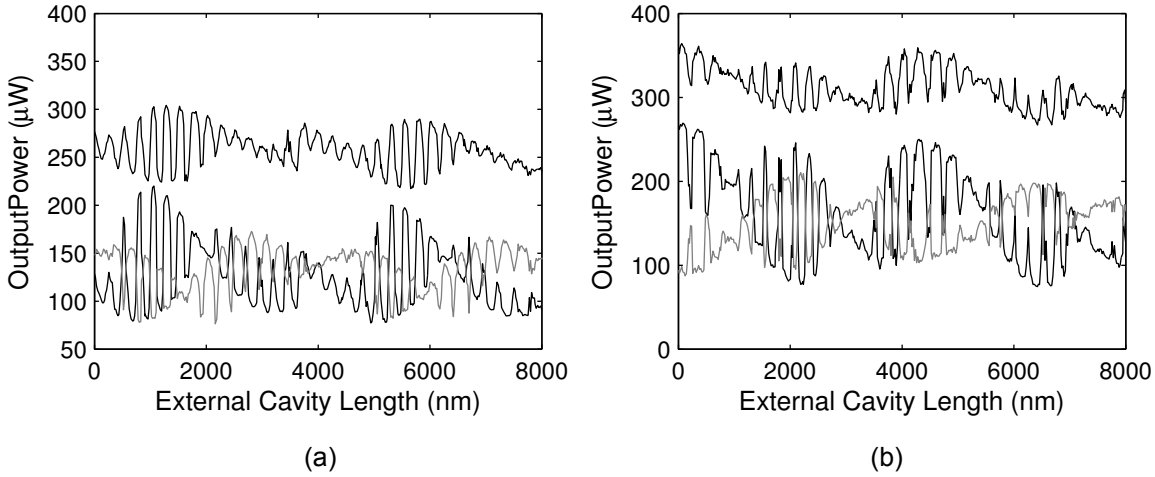

Figure 3.12: *Polarization resolved output power as a function of the ESEC length for a fixed current of 1.5 mA (a) and 2 mA (b). Grey and black lines represent both LP modes. Black line over them represents the total power.*

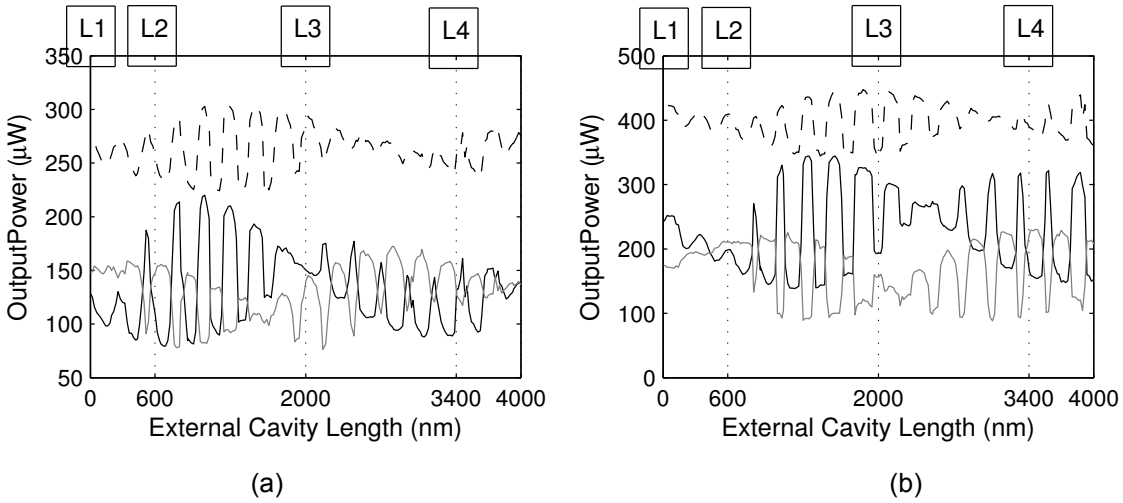

Figure 3.13: *Polarization resolved output power at different lengths of the cavity for a fixed current of 1.5 mA (a) and 2 mA (b). Grey and black lines represent both LP modes. Black line over them represents the total power.*

In Fig. 3.14 we show the light versus current curves for the distances marked in Fig. 3.13 by L_1, L_2, L_3 and L_4. We can observe that depending on the liquid crystal cavity length, we have polarization switchings at different injection currents or not. In same cases, we have several switchings between the polarization modes.

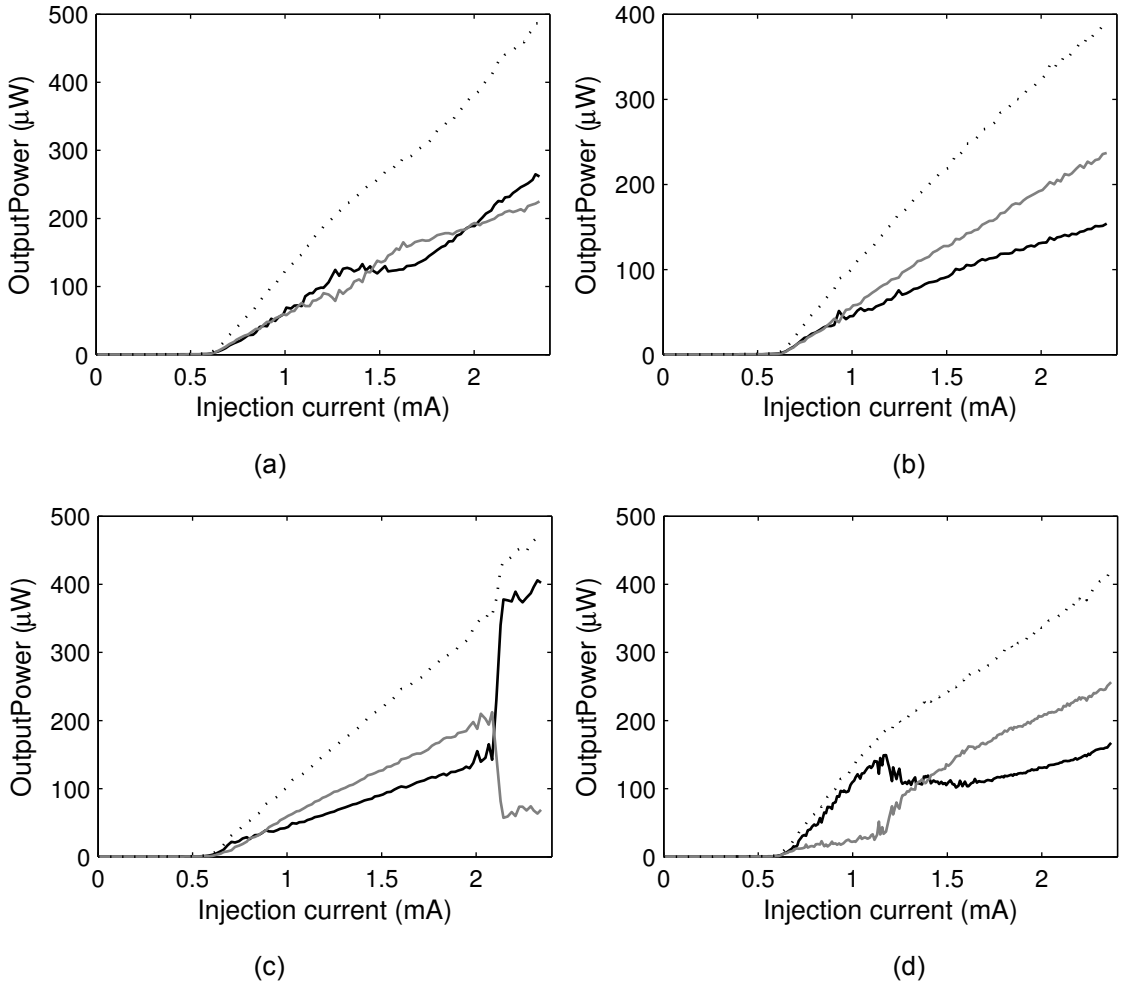

Figure 3.14: *Polarization resolved output power versus injection current for different distances: (a) 0 nm, (b) 600 nm, (c) 2000 nm, (d) 3400 nm. Grey and black lines represent both LP modes. Dashed lines represent total power.*

In the following experiments, we replace the multimode fiber with a single mode one. Fig. 3.15 shows the polarization resolved optical power versus current.

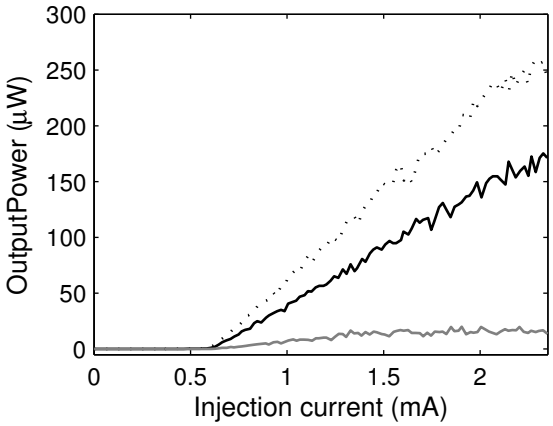

Figure 3.15: *Polarization resolved optical power versus injection current with singlemode fiber. Black and grey lines represent the two LP polarization modes. Dashed line represents the total power.*

We sweep the length of the liquid crystal cavity for fixed values of injection current measuring the optical output power. We can not observe a significant decrease of the optical power with the length of the external cavity filled in with liquid crystal as it is shown in the Fig. 3.16 for the case of 2 mA.

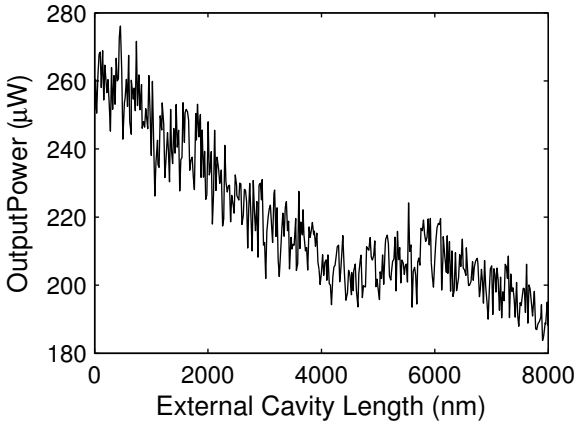

Figure 3.16: *Optical power obtained varying the LC cavity for a fixed current of 2 mA using a singlemode fiber.*

This result might be caused by a bad coupling of the singlemode fiber. It is very complicated to align it properly with the VCSEL having the liquid crystal drop, so perhaps we are not close enough to see the effects of the extremely short external cavity on the optical feedback.

Chapter 4

Conclusions and future perspectives

We carry out experiments to investigate the impact of optical feedback from ESEC filled in with liquid crystal on the characteristics of vertical cavity surface emitting lasers. First, we work extensively with an empty extremely short external cavity and experimentally investigate how optical feedback from an ESEC affects VCSELs behaviour. Our results obtained show that the total power and the wavelength of the operation of the VCSEL are modulated with a period of a half the wavelength of operation if the cavity length is varied. The amplitude of the modulation is increased when the external reflectivity increases gluing a mirror to the fiber cleaved facet.

The polarization switchings between the two orthogonal LP modes are observed with multimode optical fiber as incomplete switches and modulation of total power. We observe them more clearly when working with a singlemode fiber and controlling the polarization with a fiber polarization controller piece.

Measuring the wavelength of operation versus the injection current curve at different fixed distances, we observe that the operation wavelength shifts. The slope of the curves is the same although we change the distance

By putting a liquid crystal drop on the pedestal of the VCSEL, we create an extremely short external cavity filled in with liquid crystal. Such cavity strongly affects on the VCSELs characteristics: it increases the threshold current, decreases the VCSEL slope efficiency and makes the polarization of light not linear.

Carrying out the experiment with multimode fiber, when varying the length of the cavity, we can observe a double modulation of the power. It is modulated with a period of P_1 = 300 nm and the amplitude is also modulated with a period of $P_2 = 10 \cdot P_1$. The modulation of P_1 corresponds to the ordinary refractive index n_o of the liquid crystal. The

10 cycle modulation corresponds to the liquid crystal birefringence: $\Delta n = n_e - n_o$. This modulation is also observed in both modes of polarization that switch within each period of modulation of the total power.

Initial experiments with singlemode fiber and liquid crystal filling in the ESEC have been carried out, too.

There is a lot of work that can be done after this master thesis. First, we can investigate more into detail the effect of the polarization modulation in the VCSEL with the liquid crystal drop. Then, it would be interesting to investigate the impact of the liquid crystal on the dynamical characteristics of VCSELs. It would be also interesting to study the polarization resolved resolved light versus distance characteristics when a electro-optically driven liquid crystal is inserted in the external cavity. It would be important to study theoretically the light propagation in optically anisotropic liquid crystal medium placed between the VCSEL and reflecting features of different reflectivity, placed at different distance and to elaborate rate equation approaches typical for semiconductor lasers to take into account the presence of external resonator filled in with anisotropic medium.

With that work, we would answer the question if a liquid crystal overlay can be used for tuning the lasing properties of the VCSEL, namely tuning the optical cavity length of the VCSEL by electrically switching the liquid crystal and stabilization of the polarization state of the emitted light by using the liquid crystal anisotropy.

Bibliography

[1] L. A. Coldren and S. W. Corzine, "Diode Lasers and Photonic Integrated Circuits", John Wiley & Sons, (1995).

[2] G. P. Agrawal**,** "Fiber-Optic Communications Systems", John Wiley & Sons, 3rd Edition, (2002).

[3] A. K. Jansen van Doorn, M. P. van Exter, and J. P. Woerdman, ''Elasto-optic anisotropy and polarization orientation of vertical-cavity surface-emitting semiconductor lasers'', Appl. Phys. Lett. **69**, 1041–1043 (1996).

[4] C. J. Chang-Hasnain, J. P. Harbison, G. Hasnain, A. C. V. Lehmen, L. T. Florez, and N. G. Stoffel, "Dynamics, polarization and transverse mode characteristics of vertical cavity surface emitting lasers," IEEE J. Quant. Electr., vol. 27, no. 6, pp. 1402–1408, 1991.

[5] B. Ryvkin, K. Panajotov, A. Georgievski, J. Danckaert, M. Peeters, G. Verschaffelt, H. Thienpont, and I. Veretennicoff, "Effect of photon-energy-dependent loss and gain mechanisms on polarisation switching in vertical-cavity surface-emitting lasers", J. Opt. Soc. Am. B16, pp. 2106-2113, (1999).

[6] S. Jiang, Z.Pan, M. Dagenais, R. A. Morgan and K. Kojima, "Influence of external optical feedback on threshold and spectral characteristics of vertical-cavity surfaceemitting lasers", IEEE Photon. Technol. Lett. **6**, pp. 34-36 (1994).

[7] Y. C. Chung and Y. H. Lee, "Spectral characteristics of vertical-cavity surface emitting laser with optical feedback", IEEE Photon. Technol. Lett. 3, pp. 597-599, (1991).

[8] K. Petermann, "External optical feedback phenomena in semiconductor lasers," IEEE J. Quant. Electr., vol. 1, no. 2, pp. 480–489, 1995.

[9] M. Arizaleta, “Extremely short external cavity VCSELs: a novel approach to control polarization and to study temporal dynamics”, PhD thesis, Vrije Universiteit Brussel, Brussels, 2007.

[10] Iam-Choo Khoo**, “**Liquid Crystals”, Wiley-Interscience, 2nd Edition, (2007).

[11] C. Imrie, “The world of liquid crystals”, Royal Society of Chemistry, The age of the molecule, University of Aberdeen, pp. 161-180, 1999.

[12] Chandrasekhar, **“**Liquid Crystals”, Cambridge: Cambridge University Press, 2nd Edition, (1992).

[13] J. Otón, J.M. Sánchez Pena, F. Olarte and A. Serrano, “Mundo Electrónico”. Suplemento Nº 218, 3 (1991).

[14] P.J. Colling and M. Hird, “Introduction to Liquid Crystals”. Chemistry and Physics. Taylor and Francis. London (1997).

[15] D. Velasco Castrillo, “Mundo científico 15”, nº 162, 958 (1995).